Decline and recovery of total column ozone using a multimodel time series analysis

John Austin,[1,2] J. Scinocca,[3] D. Plummer,[4] L. Oman,[5] D. Waugh,[5] H. Akiyoshi,[6] S. Bekki,[7] P. Braesicke,[8] N. Butchart,[9] M. Chipperfield,[10] D. Cugnet,[7] M. Dameris,[11] S. Dhomse,[10] V. Eyring,[11] S. Frith,[12,13] R. R. Garcia,[14] H. Garny,[11] A. Gettelman,[14] S. C. Hardiman,[9] D. Kinnison,[14] J. F. Lamarque,[14] E. Mancini,[15] M. Marchand,[7] M. Michou,[16] O. Morgenstern,[17] T. Nakamura,[6] S. Pawson,[12] G. Pitari,[15] J. Pyle,[8] E. Rozanov,[18,19] T. G. Shepherd,[20] K. Shibata,[21] H. Teyssèdre,[16] R. J. Wilson,[1] and Y. Yamashita[6]

Received 11 January 2010; revised 1 June 2010; accepted 1 July 2010; published 4 November 2010.

[1] Simulations of 15 coupled chemistry climate models, for the period 1960–2100, are presented. The models include a detailed stratosphere, as well as including a realistic representation of the tropospheric climate. The simulations assume a consistent set of changing greenhouse gas concentrations, as well as temporally varying chlorofluorocarbon concentrations in accordance with observations for the past and expectations for the future. The ozone results are analyzed using a nonparametric additive statistical model. Comparisons are made with observations for the recent past, and the recovery of ozone, indicated by a return to 1960 and 1980 values, is investigated as a function of latitude. Although chlorine amounts are simulated to return to 1980 values by about 2050, with only weak latitudinal variations, column ozone amounts recover at different rates due to the influence of greenhouse gas changes. In the tropics, simulated peak ozone amounts occur by about 2050 and thereafter total ozone column declines. Consequently, simulated ozone does not recover to values which existed prior to the early 1980s. The results also show a distinct hemispheric asymmetry, with recovery to 1980 values in the Northern Hemisphere extratropics ahead of the chlorine return by about 20 years. In the Southern Hemisphere midlatitudes, ozone is simulated to return to 1980 levels only 10 years ahead of chlorine. In the Antarctic, annually averaged ozone recovers at about the same rate as chlorine in high latitudes and hence does not return to 1960s values until the last decade of the simulations.

Citation: Austin, J., et al. (2010), Decline and recovery of total column ozone using a multimodel time series analysis, *J. Geophys. Res.*, *115*, D00M10, doi:10.1029/2010JD013857.

1. Introduction

[2] Ozone continues to be an important atmospheric species, due to its impact on the biosphere by absorbing ultraviolet radiation, and because of its contribution to climate processes. The long-term evolution of ozone is influenced by a wide variety of factors which may be broadly separated into radiative, dynamical, transport, chemical and

[1]NOAA Geophysical Fluid Dynamics Lab., Princeton, New Jersey, USA.
[2]University Corporation for Atmospheric Research, Boulder, Colorado, USA.
[3]CCMA, University of Victoria, Victoria, British Columbia, Canada.
[4]Science and Technology Branch, Environment Canada, Toronto, Ontario, Canada.
[5]Department of Earth and Planetary Sciences, John Hopkins University, Baltimore, Maryland, USA.
[6]National Institute for Environmental Studies, Tsukuba, Japan.
[7]IPSL, UVSQ, UPMC, CNRS, INSU, Paris, France.
[8]NCAS-Climate-Chemistry, Centre for Atmospheric Science, Department of Chemistry, Cambridge University, Cambridge, UK.
[9]Hadley Centre, Met Office, Exeter, UK.
[10]School of Earth and Environment, University of Leeds, Leeds, UK.
[11]Deutsches Zentrum für Luft- und Raumfahrt, Institut für Physik der Atmosphäre, Wessling, Germany.
[12]NASA Goddard Space Flight Center, Greenbelt, Maryland, USA.
[13]Science Systems and Applications, Inc., Beltsville, Maryland, USA.
[14]NCAR, Boulder, Colorado, USA.
[15]Dipartimento di Fisica, University of L'Aquila, L'Aquila, Italy.
[16]GAME, CNRM, Meteo-France, Toulouse, France.
[17]National Institute of Water and Atmospheric Research, Lauder, New Zealand.
[18]Physical-Meteorological Observatory/World Radiation Center, Davos, Switzerland.
[19]ETH Zürich, Zurich, Switzerland.
[20]Department of Physics, University of Toronto, Toronto, Ontario, Canada.
[21]Meteorological Research Institute, Japan Meteorological Agency, Tsukuba, Japan.

Copyright 2010 by the American Geophysical Union.
0148-0227/10/2010JD013857

external forcing processes. Many of the processes are also coupled in the sense that for example dynamical changes lead to chemical changes which feed back onto the dynamics.

[3] Stratospheric temperature is influenced by radiative processes through changes in O_3 and the long-lived greenhouse gases (GHGs) [*Shine et al.*, 2003], primarily CO_2. As well as influencing the rates of chemical reactions, the stratospheric temperature controls the formation of polar stratospheric clouds, which are implicated in polar ozone destruction [e.g., *Solomon*, 1999]. In turn, horizontal temperature gradients affect the propagation of Rossby waves which contribute to the Brewer-Dobson circulation, and on climate time scales this leads to increased transport of atmospheric constituents [*Butchart and Scaife*, 2001] from the tropics to the poles.

[4] In model simulations, ozone amounts are influenced by both resolved and parameterized wave forcing. Resolved waves include synoptic scale and planetary waves, which determine the strength of the winds in the polar vortex. Most models include parameterizations for both orographic and nonorographic gravity waves which are crucial to simulate realistic polar vortex strength. For those models which have sufficient vertical resolution, a spontaneous quasi-biennial oscillation (QBO) [*Takahashi*, 1996] can occur. The QBO is an important part of the tropical variability, but also contributes to interannual variability in high-latitude stratospheric winds by the well-known Holton-Tan effect [*Holton and Tan*, 1980]. Wave processes have a direct effect on ozone amounts through transport. Dynamical processes also influence temperatures which in turn affect the chemistry of ozone because of the temperature dependence of the reaction rates.

[5] The net ozone change is essentially the balance between transport and chemistry. Changes in the Brewer-Dobson circulation [*Shepherd*, 2008] can have important direct effects on ozone as well as influencing the concentrations of long-lived species, especially Cl_y and NO_y, which produce further chemical changes [*Douglass et al.*, 2008].

[6] Chemical influences on ozone have been dominated in recent decades by the halogen loading [*Eyring et al.*, 2006], and this will also likely remain the focus of attention for several decades to come. While chlorine remains present in high concentrations in the atmosphere, volcanic eruptions could play an important role through the supply of sites for heterogeneous reactions [*Tie and Brasseur*, 1995]. Changes in water vapor concentration from for example CH_4 oxidation, change the concentration of HO_x radicals and in the amount of polar stratospheric clouds (PSCs). HO_x catalytically destroys ozone and changes the balance of other chemical species. Chemical effects also arise from N_2O increases, which lead to increased NO_y, and future ozone loss [*Portmann and Solomon*, 2007].

[7] Water vapor concentrations in the stratosphere depend on the tropical tropopause temperature, and convection processes in the tropics. The region is also a source of very short lived species which contribute to ozone depletion [*World Meteorological Organization* (*WMO*), 2007, chapter 2].

[8] The degree to which the combined effect of these factors influences the future evolution of ozone is investigated in this paper. One of the most effective ways to investigate ozone trends is using results from a set of coupled chemistry climate models (CCMs), with well-resolved stratospheres. These are now capable of representing in detail most of the processes alluded to above. This paper extends the line of similar investigations [*Austin et al.*, 2003; *Eyring et al.*, 2007] on the analysis of previous model intercomparisons for the stratosphere. *Oman et al.* [2010] also analyze the results of the same model simulations using linear regression to try to quantify the factors responsible for the ozone changes.

[9] A focus of this study is the timing of ozone recovery and we concentrate essentially on total column ozone because it is one of the dominant factors affecting the surface UV flux. In the 2006 ozone assessment [*WMO*, 2007] ozone recovery is expressed in terms of ozone increase relating to a reduction in ozone depleting substances (ODSs). Here, we consider a more generalized ozone recovery, which takes account of changes in GHGs as well. In this respect, ozone recovery can be considered in the same way as tropospheric temperature change and attribution analyses undertaken to determine the cause of ozone recovery, whether it is chemical (via ODS reduction for example), radiative (via temperature change on the reaction rates) or dynamical (via changes in transport). Hence, we use the term "ozone recovery" to imply the process of an increase in ozone from its current low levels. We avoid terms such as "full recovery" and "super recovery" which imply the need for an ozone or ODS benchmark. Instead, we refer to points along the path of ozone increase as "recovery to 1980 levels" or "return to 1980 levels." We also consider other time frames, such as ozone return to 1960 levels, which reflects the loss of ozone that likely occurred prior to the availability of extensive satellite measurements of ozone. For comparison purposes we also refer to the "return of chlorine amounts" to values present on for example 1960 and 1980.

2. Models and Simulations

[10] The list of models included in this analysis is given in Table 1. Descriptions of the models is given by *Morgenstern et al.* [2010], and model details may be found therein. The evolution of ozone is investigated using the simulations of Chemistry Climate Model Validation-2 (CCMVal-2), described by *Eyring et al.* [2008] and *Morgenstern et al.* [2010]. The set of results from experiment REF-B2 is used. In REF-B2, the simulations were used to investigate the likely behavior of stratospheric ozone for the GHG scenario A1B [*Intergovernmental Panel on Climate Change* (*IPCC*), 2001, Appendix II] and the halogen scenario A1 from *WMO* [2007, Table 8-5], with modifications described by *Eyring et al.* [2008] and *Morgenstern et al.* [2010]. All models that participated in CCMVal-2 were run seamlessly over the full period from 1960 to 2100 except E39CA, UMUKCA-METO, and GEOSCCM. In the case of E39CA and UMUKCA-METO the REF-B2 runs ended earlier (2050 and 2083, respectively). For each CCM, SSTs were taken from the coupled ocean-atmosphere results previously obtained with A1B forcings for the underlying climate model, except for CMAM which itself had a coupled ocean. Also, for GEOSCCM, for which the REF-B2 experiment started in 2000, results for the period 1960–2000 were

Table 1. List of Models Contributing to This Study

Model	Reference
AMTRAC3	*Austin and Wilson* [2010]
CAM3.5	*Lamarque et al.* [2008]
CCSRNIES	*Akiyoshi et al.* [2009]
CMAM	*Scinocca et al.* [2008]; *de Grandpré et al.* [2000]
CNRM-ACM	*Déqué* [2007]; *Teyssèdre et al.* [2007]
E39CA	*Stenke et al.* [2009]; *Garny et al.* [2009]
GEOSCCM	*Pawson et al.* [2008]
LMDZrepro	*Jourdain et al.* [2008]
MRI	*Shibata and Deushi* [2008]
SOCOL	*Schraner et al.* [2008]
ULAQ	*Pitari et al.* [2002]
UMSLIMCAT	*Tian and Chipperfield* [2005]
UMUKCA-METO	*Morgenstern et al.* [2009]
UMUKCA-UCAM	*Morgenstern et al.* [2009]
WACCM	*Garcia et al.* [2007]

included from experiment REF-B1, in which sea surface temperatures and external forcing parameters including the solar cycle, were specified from observations. Combining the two experiments did not produce an appreciable influence on the results of the analysis. The CCMVal-1 simulations used here are described by *Eyring et al.* [2006, 2007] and contributed to the 2006 Ozone Assessment [*WMO*, 2007, chapters 5 and 6]. The simulations typically covered the period 1980–2050 with realistically varying GHG and halogen amounts.

[11] The results were found to depend broadly on latitude and hence it is most natural to divide the results into mid-latitude, tropical, and polar regions. For each of these regions the objective of this paper is to present the projected past and future total column ozone change from the new (CCMVal-2) CCM simulations and to compare this with the projected ozone change from the previous (CCMVal-1) CCM simulations. We also investigate the timing of ozone recovery from the individual model results and the multimodel mean.

3. Analysis Method

[12] Ideally, a comparison between CCMVal-1 and CCMVal-2 projections would be based on analyses that produced quantitative predictions and uncertainty estimates of ozone and ozone related indices. In previous studies, time series analyses of CCMVal simulations [*WMO*, 2007; *Eyring et al.*, 2007] have provided mostly qualitative results making it difficult to formulate and use multimodel projections. Here, we use a new analysis procedure based on a statistical framework that employs a nonparametric additive model to estimate individual-model trends (IMT) and multimodel trends (MMT). The method is described in detail by *Scinocca et al.* [2010], along with examples of its application to the CCMVal-1 data, and is referred to as the Time-Series Additive Model (TSAM).

[13] In section 4, the TSAM analysis is applied to both the CCMVal-1 and current CCMVal-2 total column ozone and 50 hPa total inorganic chlorine to identify any changes or improvements in model simulations since the work of *Eyring et al.* [2007]. Several of the CCMVal-1 results presented here are also shown by *Scinocca et al.* [2010]. The final MMT estimates are suitable for the production of multimodel estimates of return dates and this is discussed in section 5. As in work by *Scinocca et al.* [2010], the TSAM analysis used here assumes equal weighting of each model. Alternative weightings have been explored, but for reasons discussed in section 6, are not considered further.

4. Results

4.1. Tropical Ozone

[14] Figure 1 (left) shows the raw time series data and the initial TSAM individual-model trend (IMT) estimates for the annual total column ozone in the latitude band 25°S–25°N for 11 CCMVal-1 models (Figure 1, top left) and 13 CCMVal-2 models (Figure 1, bottom left). These initial IMT estimates employ the nonparametric additive model discussed by *Scinocca et al.* [2010] and were verified by an analysis of the residuals, which were found to be normally distributed about 0. Observations of total ozone from four data sets are also presented in Figure 1 (black lines and symbols). These include ground-based measurements (updated from *Fioletov et al.* [2002]), merged satellite data [*Stolarski and Frith*, 2006], the National Institute of Water and Atmospheric Research (NIWA) combined total column ozone database [*Bodeker et al.*, 2005], and Solar Backscatter Ultraviolet (SBUV, SBUV/2) retrievals (updated from *Miller et al.* [2002]). The observational data sets have been combined using the TSAM analysis to provide a single observed time series.

[15] Over the entire period of the CCMVal-1 results, both the CCMVal-1 and CCMVal-2 time series display a wide range of background total ozone values, which extend significantly above and below the observed values in this region. While the biases of most models have remained unchanged between the two intercomparison projects, two models show significant differences from CCMVal-1 to CCMVal-2: WACCM has changed from a positive bias to a negative bias and UMSLIMCAT has changed from a near zero bias to a significant negative bias.

[16] As described by *Scinocca et al.* [2010], relative to a selected reference date, baseline-adjusted time series and IMT estimates are computed in the second step of the TSAM analysis to facilitate a closer comparison of the predicted evolution of ozone indices between models. Analogous to the analysis performed by *WMO* [2007, chapter 6] and *Eyring et al.* [2007], anomaly time series are created for each model about a baseline value. Here, the baseline value is taken to be the initial IMT estimate at a selected reference date for each model (e.g., 1980). The baseline adjusted time series are then formed by adding a constant so that each anomaly time series goes through the multimodel average of the IMT estimates at the reference date. Since the multimodel average of the IMT estimates is a close approximation to the final multimodel trend estimate (MMT) derived in the third step of the TSAM analysis, the baseline adjustment may be viewed simply as forcing the anomaly time series to go roughly through the final MMT estimate at the reference date.

[17] The baseline-adjusted IMT estimates employing a reference date of 1980 are presented in Figure 1 (right). Comparing Figure 1 (left) and Figure 1 (right) it can be seen

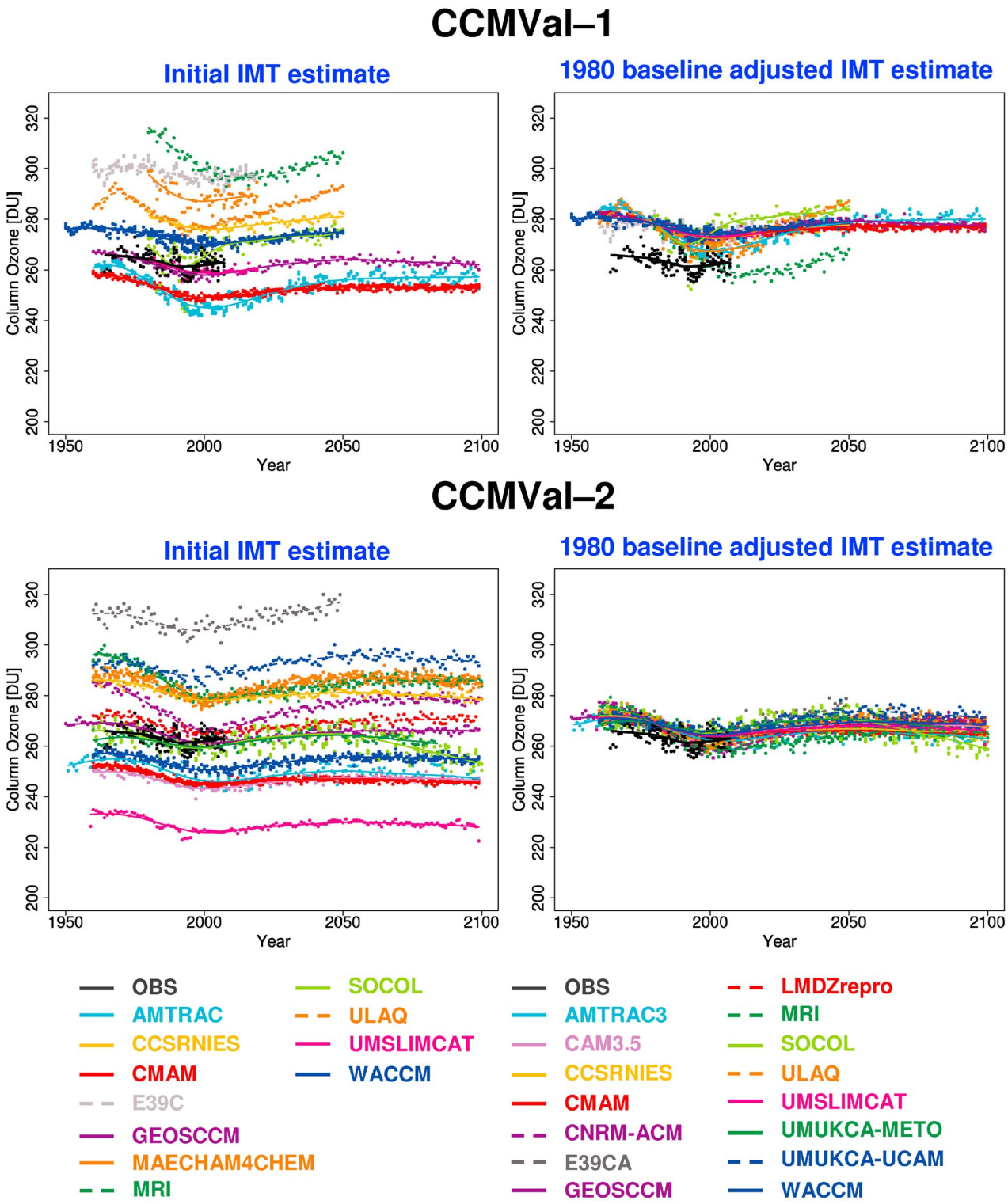

Figure 1. (left) Raw time series data of annually averaged total ozone for the latitude range 25°S–25°N and initial individual model trend (IMT) estimates and (right) 1980 baseline-adjusted time series data and 1980 baseline-adjusted IMT estimates for the TSAM analysis of (top) CCMVal-1 and (bottom) CCMVal-2. Observations are shown in black for four observational data sets (see text). A lowess fit (with smoother span f = 0.4) to the observations appears as a black line in all panels. The observations are not baseline-adjusted in Figure 1 (right).

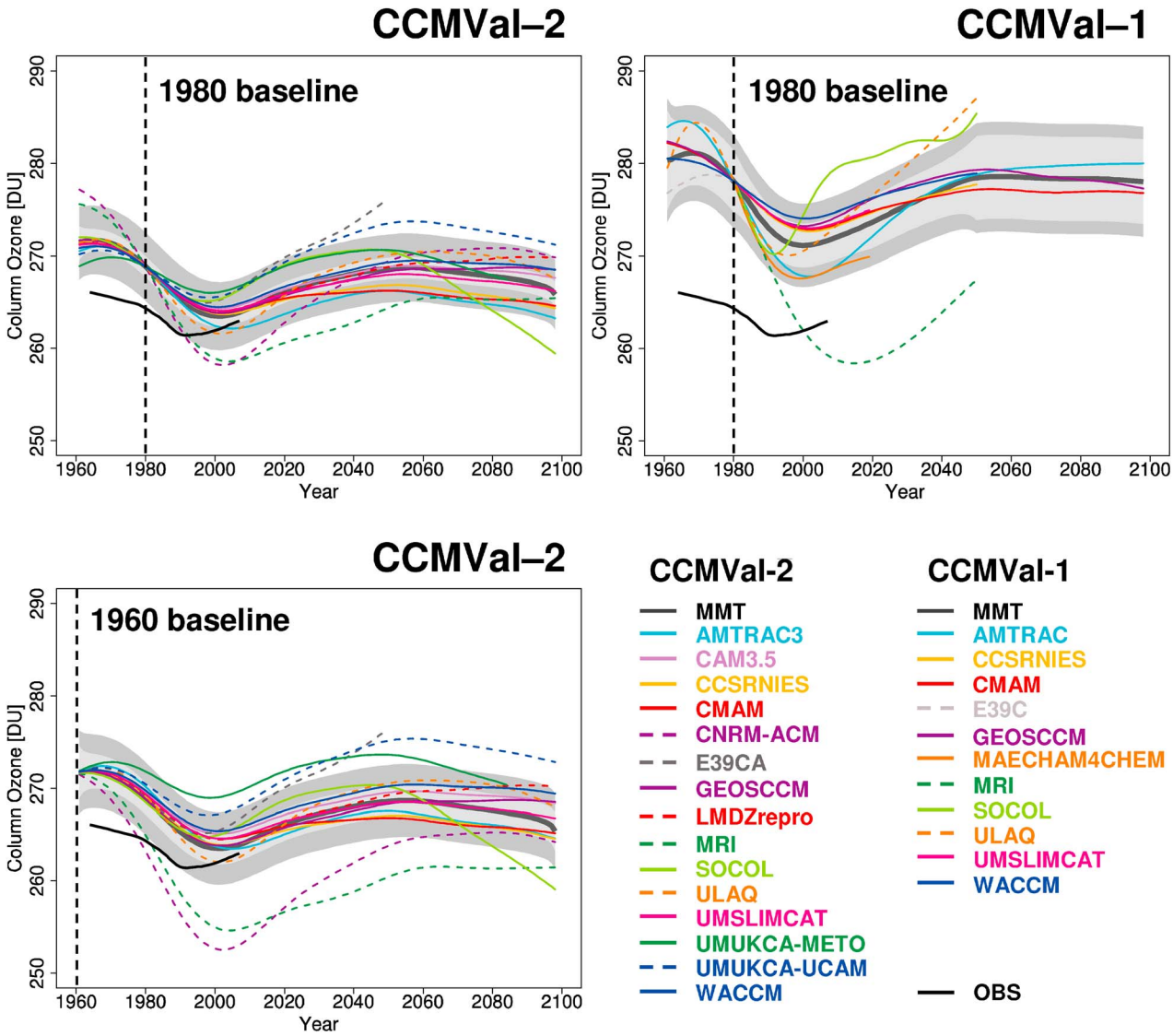

Figure 2. (top) The 1980 baseline-adjusted multimodel trend (MMT) estimates of annually averaged total ozone for the latitude range 25°S–25°N (heavy dark gray line) with 95% confidence and 95% prediction intervals appearing as light- and dark-gray shaded regions about the trend. The baseline-adjusted IMT estimates, and unadjusted lowess fit to the observations are additionally plotted. (left) CCMVal-2 results and (RIGHT) CCMVal-1 results. (bottom) The same analysis of CCMVal-2 data but for a baseline adjustment employing a 1960 reference date.

that the TSAM analysis has been very effective at providing a common reference for the total ozone time series allowing a clearer comparison of the predicted evolution between models. The baseline adjusted time series employing a reference date of 1980 show improved agreement with observations for CCMVal-2 relative to CCMVal-1. From Figure 1 (left) it can be seen that this improvement in CCMVal-2 is fortuitous in that it has not come from a reduction in the spread of models but rather through a more even spread about the observations.

[18] The 1980 baseline adjusted multimodel trend (MMT) estimates (thick grey line) computed in the final step of the TSAM analysis for the 25°S–25°N total column ozone are presented in Figure 2 (top) for CCMVal-2 (Figure 2, top left) and CCMVal-1 (Figure 2, top right). The 95% confidence and 95% prediction intervals for the MMT estimate are also displayed in Figure 2 (top) as the light and dark gray shaded intervals, respectively, and the IMT estimates are superposed on top of the MMT estimate. A comparison of the MMT estimates in Figure 2 (top) reveals a reduced error and closer agreement with the observations for CCMVal-2 relative to CCMVal-1. The tighter confidence intervals for the CCMVal-2 MMT estimate have two sources. First, more models in CCMVal-2 submitted data that extended over a greater portion of the requested period (1960–2100). Second, based on a smaller difference between the unadjusted

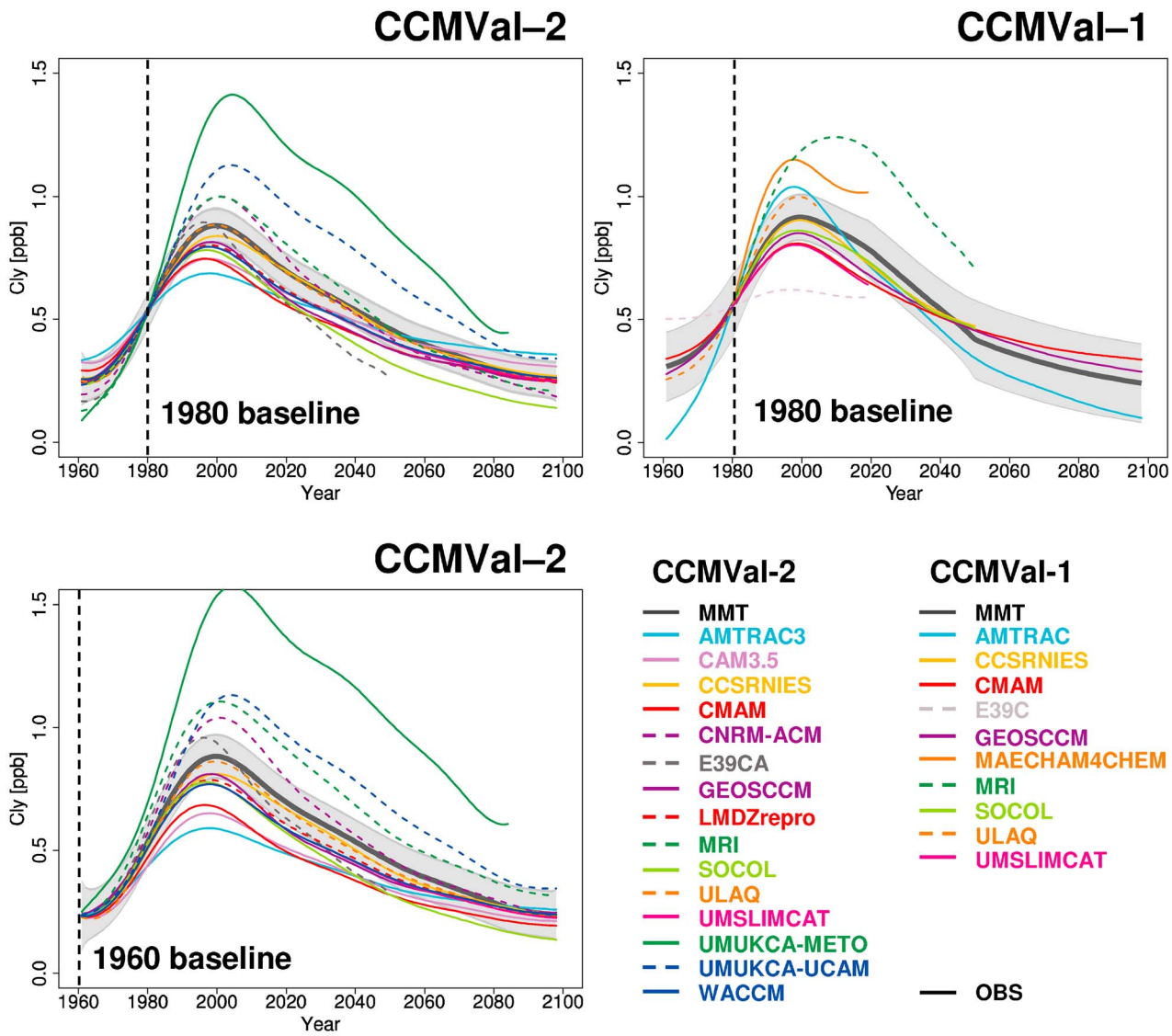

Figure 3. Same as Figure 2 but for the Cl_y amounts.

IMT and observations [see *Scinocca et al.*, 2010] several models (e.g., AMTRAC3, CCSRNIES, MRI and WACCM) have improved. For example, in AMTRAC3 the improvements have arisen from the reduction in lower stratospheric chlorine [*Austin and Wilson*, 2010].

[19] The MMT estimates in Figure 2 (top) indicate that the evolution of total ozone in the tropics is relatively unchanged between the CCMVal-1 and CCMVal-2 data sets. There is a general decline from the start of the integrations until about the year 2000. By this time, the TSAM analysis of the observations (black line) is already increasing, but this is not statistically significant and more data are needed before the timing of the minimum can be accurately established. Following a gradual increase until about 2050, simulated column ozone amounts decline slightly toward the end of the century. However, after the year 2000, the secular variation in annual mean tropical ozone is only about 10 DU. Increased transport by the Brewer-Dobson circulation is likely one of the largest drivers [*Shepherd*, 2008; *Li et al.*, 2009], and chlorine only has a small influence. The corresponding TSAM analysis of the 50 hPa Cl_y is shown in Figure 3. For CCMVal-1, MRI is a high outlier and E39C is a low outlier, as noted by *Eyring et al.* [2007]. The rates of change of chlorine in the separate models also varies, which in combination with the change in the number of models included leads to a noticeable change in gradient in the MMT curve near 2050. For CCMVal-2 there is also a wide spread in the individual IMT curves, largely due to the simulations of just a few models (AMTRAC3 and SOCOL on the low side, and the UMUKCA pair on the high side). The AMTRAC3 bias arises from an inaccurate parameterization of the halogen rate of change in the upward branch of the Brewer-Dobson circulation. The high bias in UMUKCA-METO arises from the neglect of rainout in the troposphere. Overall, though, the models are more consistent in their trends, leading to a narrower uncertainty range for the MMT.

[20] The impact of using the earlier reference date of 1960 for the baseline adjustments is shown in Figures 2 (bottom)

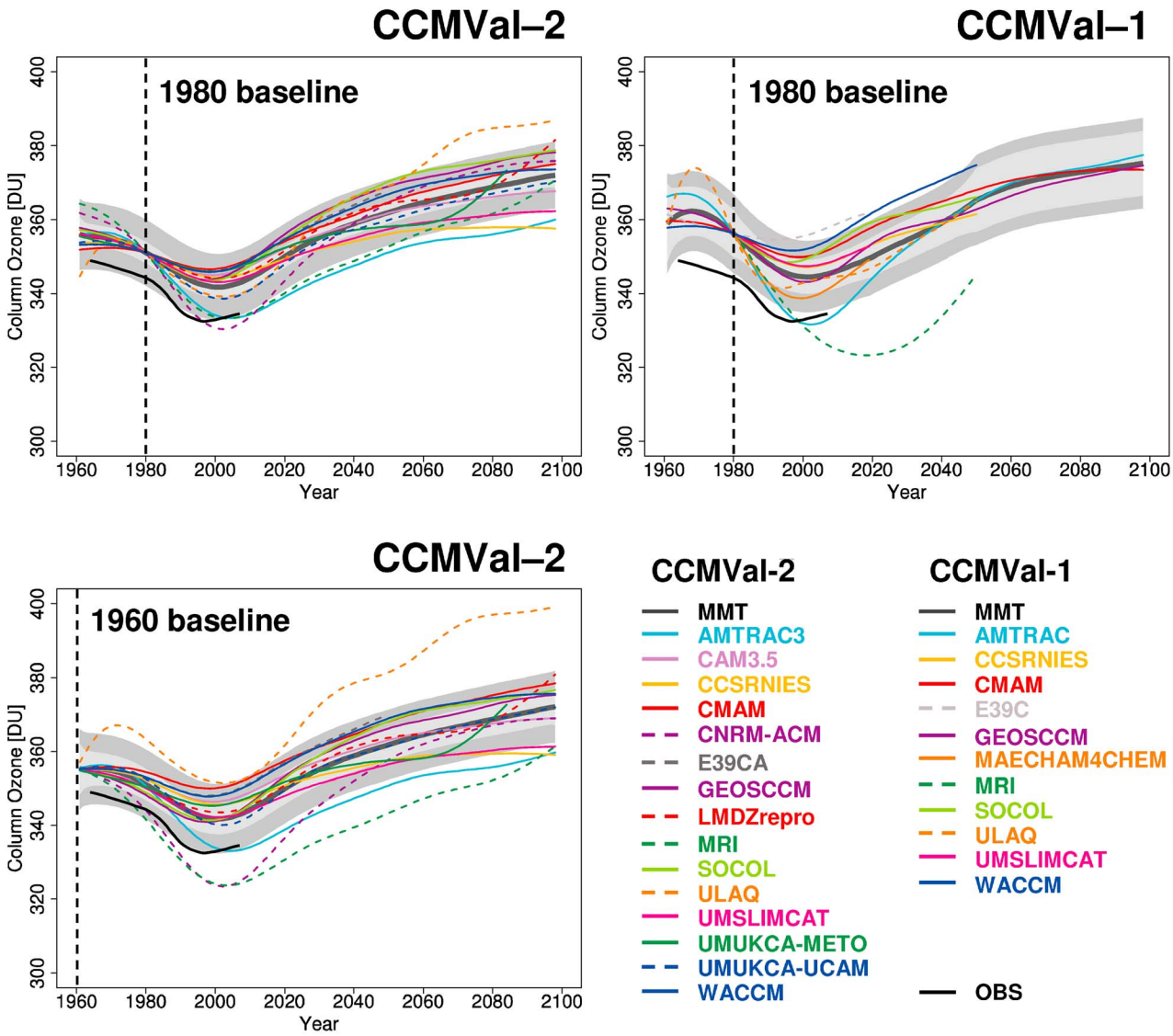

Figure 4. Same as Figure 2 but for the latitude range 35°N–60°N.

and 3 (bottom). This is only possible for the CCMVal-2 data because of their earlier starting date. It can be seen that the use of an earlier reference date for the baseline causes a significant increase in the spread of the anomaly time series particularly at the time of maximum ozone depletion. Since models with larger ozone trends from 1960–1980 also typically have larger trends from 1980–2000, choosing a 1980 baseline tends to cut the model spread at 2000 in half compared with using a 1960 baseline. In particular, the use of 1960 causes the MRI and CNRM-ACM to be larger outliers having excessive ozone depletion in all years. SOCOL is an outlier for both 1960 and 1980 baselines after about 2050. This is due to the Brewer-Dobson circulation and trend being particularly large in that model [*Oman et al.*, 2010].

4.2. Midlatitude Ozone

[21] In Figures 4 and 5, the 1980 baseline adjusted IMT and MMT estimates of total column ozone in the latitude bands 35°N–60°N and 35°S–60°S are presented for CCMVal-2 (top left) and CCMVal-1 (top right), respectively. These indicate that the multimodel average of total ozone in CCMVal-1 is generally larger than the observations in these latitude bands. While the multimodel average of CCMVal-2 more closely corresponds to observations, the raw time series data (not shown) for both CCMVal-1 and CCMVal-2 show a broad background of total ozone for both hemispheres which spans the range of observations (not shown). In both hemispheres the 1980 baseline-adjusted MMT estimates of ozone indicate that the ozone minimum is reached by about the year 2000 and that ozone increases steadily and significantly thereafter.

[22] Those models which were low outliers in CCMVal-1 for southern latitudes (AMTRAC and MRI) are now more consistent with the other models, although they are still at the low end of the range of model results. Nonetheless, these models are consistent with observations from 1980 onward.

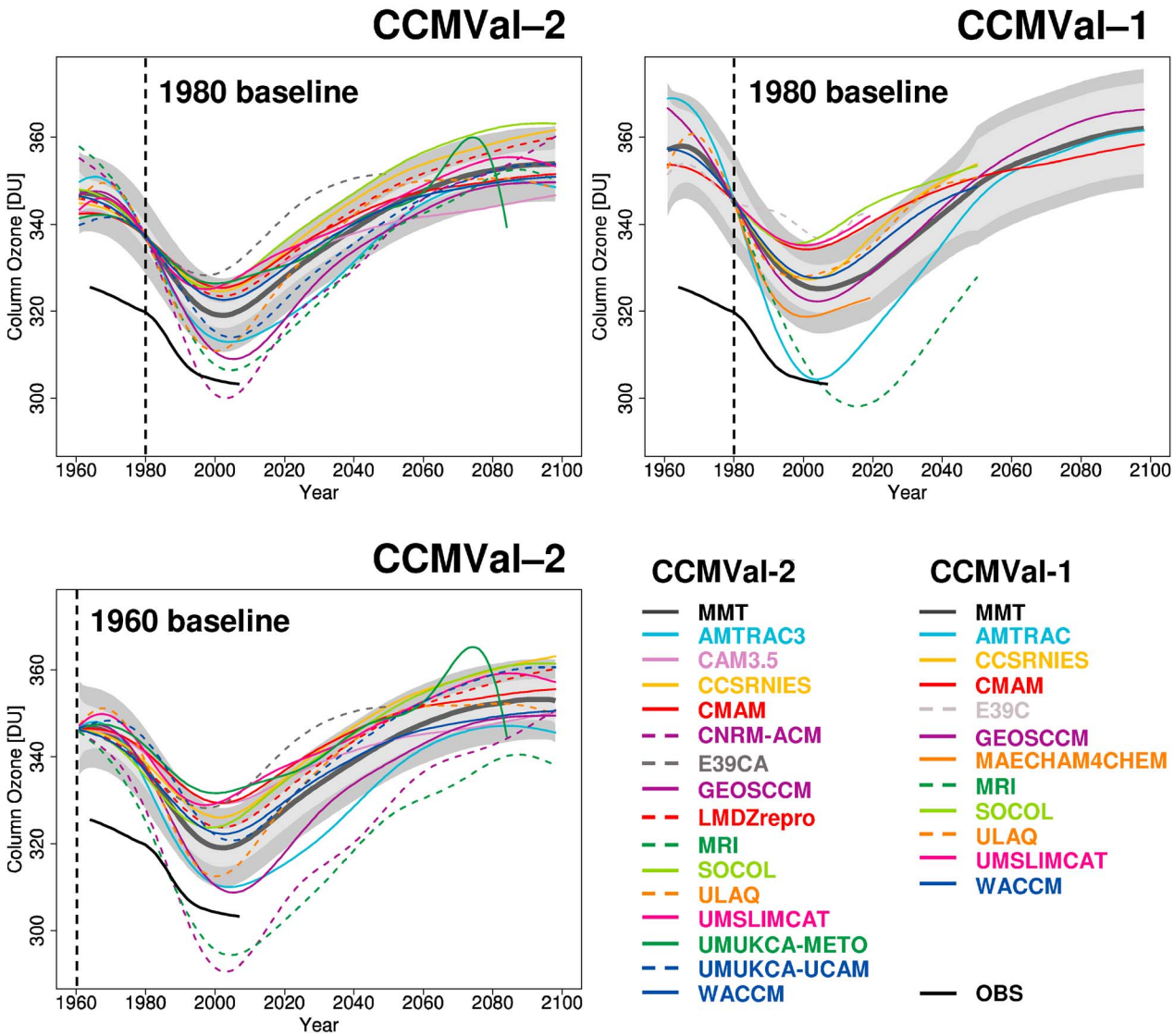

Figure 5. Same as Figure 2 but for the latitude range 35°S–60°S.

E39CA has higher values than other models for CCMVal-2 in southern midlatitudes after baseline adjustment. This is likely related to the Antarctic results (section 4.3).

[23] In Figures 4 (bottom) and 5 (bottom) the TSAM analysis of midlatitude ozone employing a 1960 baseline adjustment is presented. As in the tropics, the use of the earlier reference date significantly accentuates outliers in the trend estimates. For example, in both latitude bands, CNRM-ACM and MRI are significantly low outliers while, in northern latitudes, ULAQ appears as a significant high outlier with values that greatly exceed all models during the entire period.

[24] In Figure 6 the TSAM analysis for Northern Hemisphere midlatitude 50 hPa inorganic chlorine (Cl_y) is presented. The Southern Hemisphere Cl_y is very similar and is therefore not shown. Again, there is a large spread in Cl_y which maximizes near the year 2000. The spread between models in CCMVal-1 and CCMVal-2 is roughly equivalent, with each having several outliers. The most significant outlier in the CCMVal-2 set is UMUKCA-METO, which has excessive Cl_y in both hemispheres for all years. While the evolution of ozone generally follows that of chlorine (see section 5), the specific behavior of Cl_y for each model does not appear to account for the outliers of total column ozone identified in Figures 4 and 5.

4.3. Polar Ozone

[25] In Antarctic spring, the raw time series indicate that the range of model results has increased from CCMVal-1 to CCMVal-2 (Figure 7). This is associated with a slightly increased negative bias of CMAM relative to its CCMVal-1 contribution, and the inclusion of UMUKCA-UCAM and CAM3.5, which have large positive biases relative to the multimodel mean. In the Arctic spring, relative to CCMVal-1,

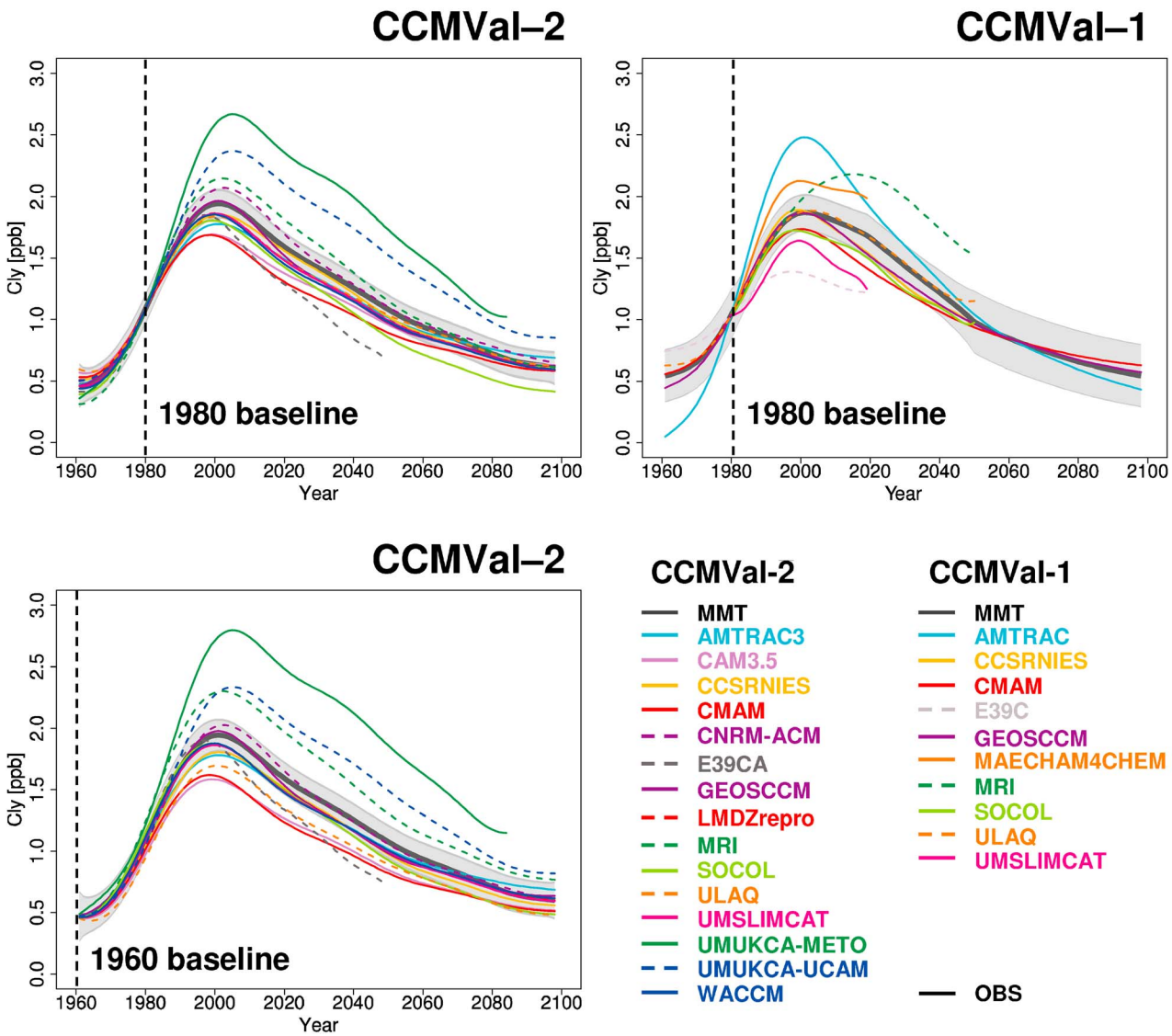

Figure 6. Same as Figure 2 but for 50 hPa Cl_y in the latitude range 35°N–60°N.

CCMVal-2 results also show no tendency toward a reduction in model spread (not shown).

[26] The TSAM analyses of spring total column ozone over the polar latitudes (60°N–90°N in March and 60°S–90°S in October) are presented in Figures 8 and 9. In the baseline adjusted time series and IMT estimates, the intermodel differences are considerably reduced compared with the raw data, especially for Antarctica. A comparison of the 1980 baseline-adjusted IMT and MMT estimates between CCMVal-1 and CCMVal-2 shows a similar convergence of the models' evolution once the offset in background values of ozone is accounted for (Figures 8 (top) and 9 (top), aside from MRI in CCMVal-1).

[27] As was the case for the other latitude bands, employing the earlier reference date of 1960 for the TSAM analysis results in larger intermodel spread for both the Arctic and Antarctic column ozone (Figures 8 (bottom left) and 9 (bottom left)). Similar to the behavior in northern midlatitudes, in the Arctic, MRI is a low-ozone outlier during nearly the entire period (Figure 8). In the Antarctic, the use of the earlier 1960 reference date increases the low bias of GEOSCCM, MRI, and AMTRAC3 and the high bias of CAM3.5, CCSRNIES, and UMUKCA-METO near 2000. A comparison of the Arctic and Antarctic spring ozone in Figures 8 and 9 indicates the tendency for Arctic ozone to recover earlier than the Antarctic (see section 5).

[28] The results for polar regions, particularly Antarctica, are dominated by chlorine amounts. The IMT and MMT estimates of annual 50 hPa Cl_y over polar latitudes (60°N–90°N and 60°S–90°S) are presented in Figures 10 and 11. Aside from the introduction of UMUKCA-METO and perhaps UMUKCA-UCAM, the CCMVal-2 50 hPa Cl_y at both poles shows less spread than CCMVal-1 when a 1980 baseline is employed (Figures 8 (top) and 9 (top)). This is primarily associated with improvement in AMTRAC and the absence of MAECHAM4CHEM. These annual means are

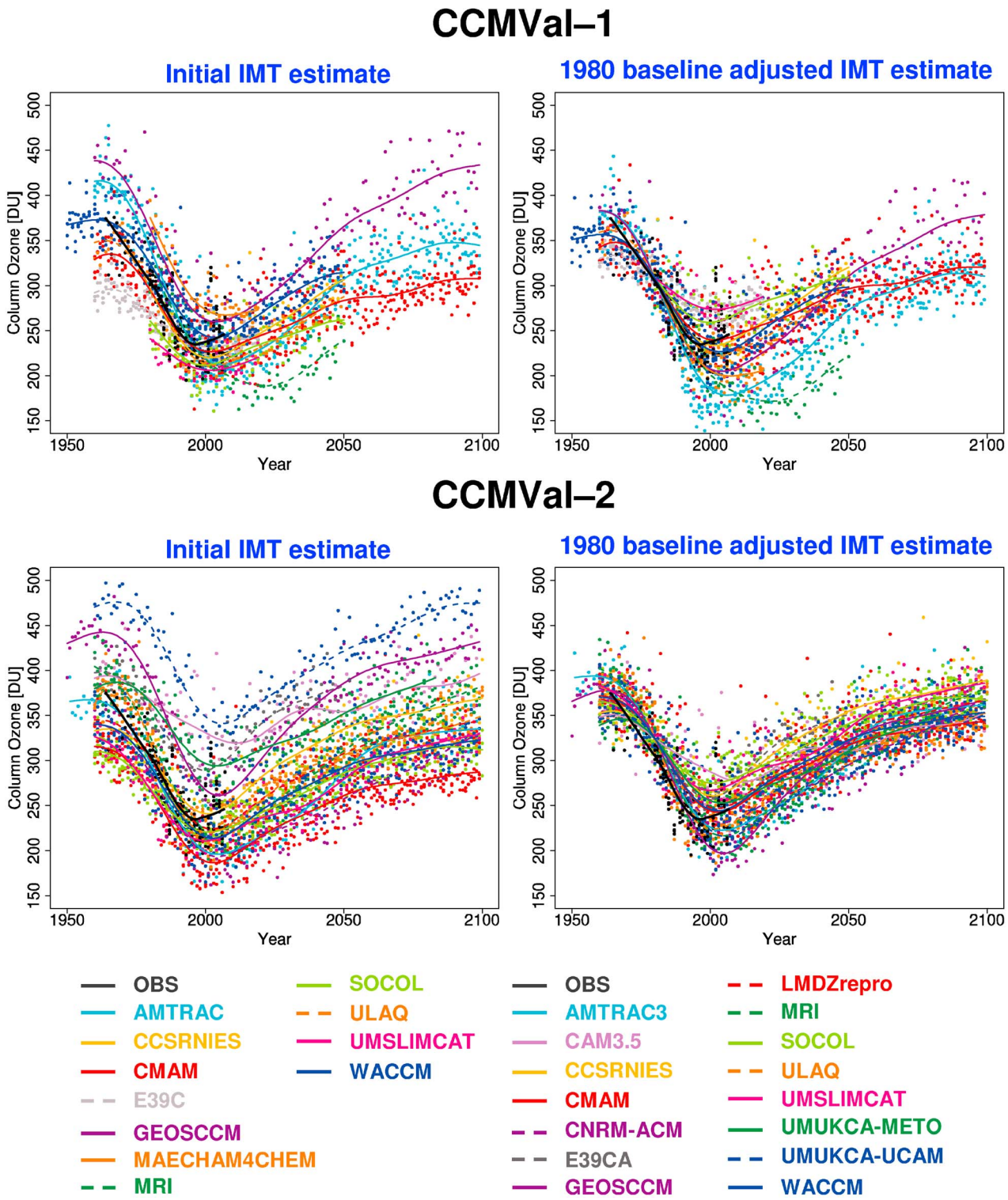

Figure 7. Same as Figure 1 but for the month of October and the latitude range 60°S–90°S.

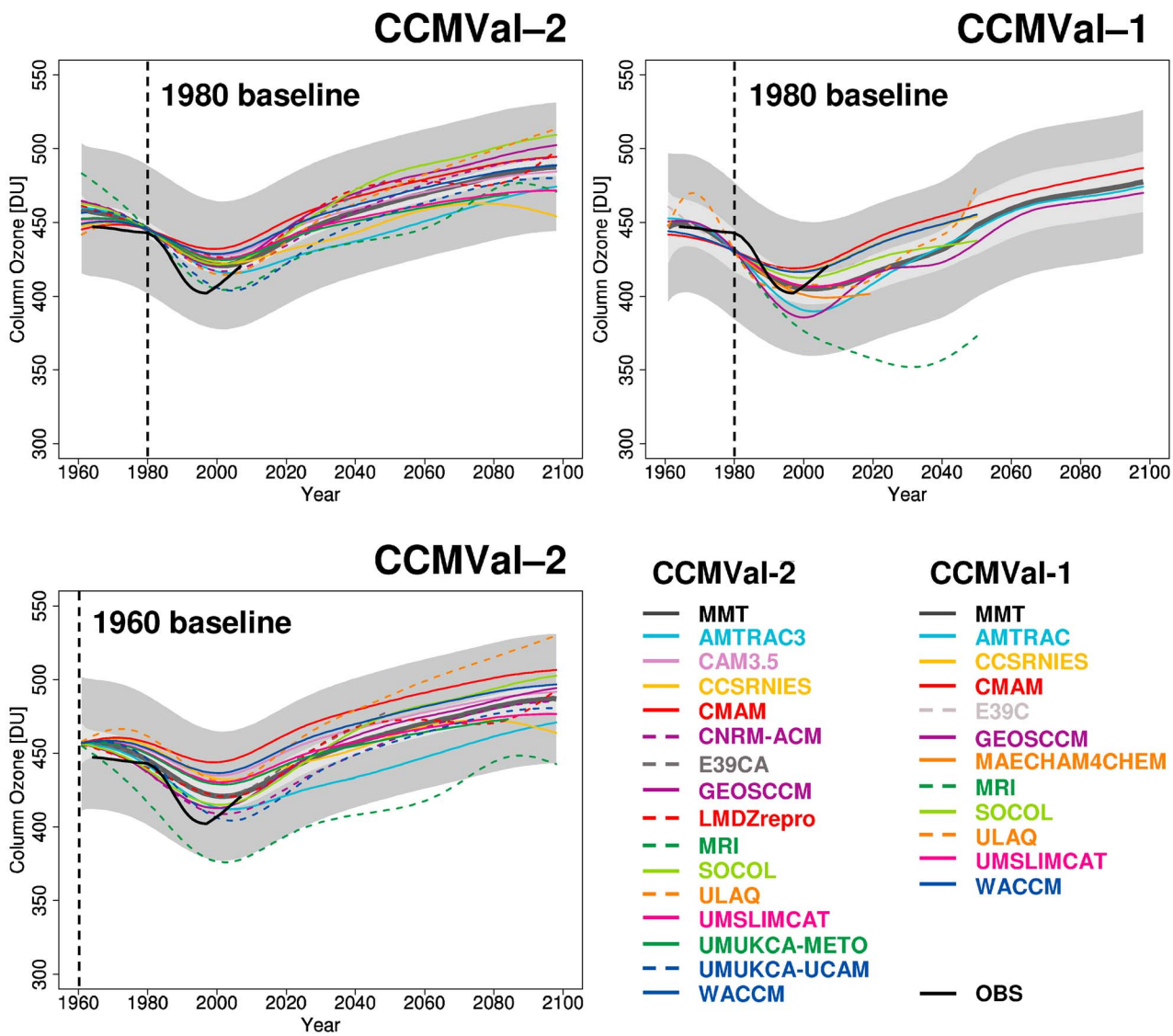

Figure 8. Same as Figure 2 but for the month of March and the latitude range 60°N–90°N.

very similar to the spring means (not shown) in both the Arctic and Antarctic. Unlike ozone, the use of a 1960 baseline in the derivation of the IMT and MMT estimates does not lead to a significant increase in model spread.

[29] Further analysis of the simulated Antarctic ozone holes is presented by *Austin et al.* [2010].

5. Ozone Recovery

5.1. TSAM Analysis

[30] The IMT and MMT estimates for total ozone and 50 hPa Cl_y presented in section 4 may be used to provide individual model, and multimodel estimates of the return to levels associated with a specified reference date. Because the IMT and MMT estimates are smooth curves by construction, the value of ozone and Cl_y for any reference date prior to maximum ozone depletion may be mapped onto a future date based on the return of ozone or Cl_y to the reference date value. In order to compare recovery predictions from CCMVal-1 with CCMVal-2, we first consider the commonly used reference date of 1980.

[31] Total ozone and 50 hPa Cl_y 1980 return dates are presented in Figures 12 and 13, respectively, for the latitude bands discussed in section 4. In each latitude band, CCMVal-1 return dates are shown on the left and CCMVal-2 return dates are shown on the right. The MMT estimate of return dates is indicated by large black triangles. Error bars on these estimates are associated with the 95% confidence intervals. Figures 12 and 13 provide a concise summary of the ozone and Cl_y discussed in section 4. They allow an overall comparison of CCMVal-1 with CCMVal-2 through the MMT estimates, the change in individual model predictions to be tracked across the two intercomparison projects, and the comparison of model predictions with the MMT estimates and with each other for each of CCMVal-1 and CCMVal-2.

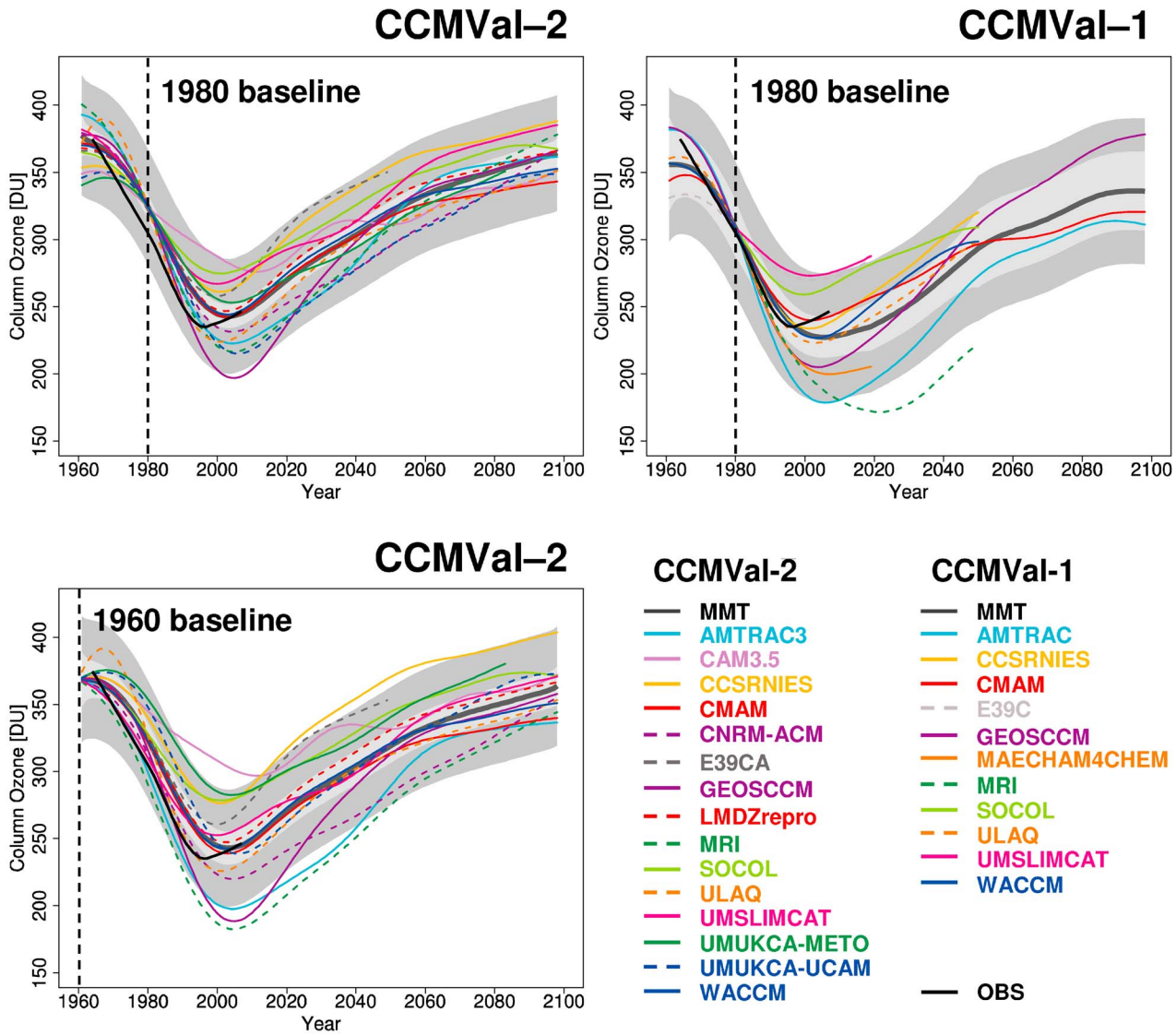

Figure 9. Same as Figure 2 but for the month of October and the latitude range 60°S–90°S.

[32] The return dates for Cl_y (Figure 13) are more symmetric in latitude, and more certain, than ozone (Figure 12) for both CCMVal-1 and CCMVal-2. In general, return dates for Cl_y are very similar in CCMVal-1 and CCMVal-2 and are well within the uncertainty bounds of each other. By contrast, return dates for total ozone are not symmetric in latitude, and, in the tropics for CCMVal-2, the MMT ozone does not return to 1980 values. In general, CCMVal-2 ozone return dates are systematically earlier than in CCMVal-1, although the difference is not statistically significant. For example, the spring Arctic ozone recovery to 1980 levels is predicted from the MMT estimate to occur near 2025 for CCMVal-2 (2039 for CCMVal-1) while the Antarctic recovery to 1980 levels is predicted to occur much later near 2052 for CCMVal-2 (2062 for CCMVal-1). The asymmetric structure of polar ozone recovery in Figure 12 is an indication that, in addition to Cl_y abundance, ozone is affected by dynamical and radiative changes induced by increased GHG forcing which have been consistently reproduced in the MMT estimates between CCMVal-1 and CCMVal-2.

[33] In Figures 14 and 15 we compare estimates of the return dates to 1960 and 1980 levels for total ozone and 50 hPa Cl_y, respectively. For Antarctica the return date changes significantly from about 2055 (1980 return) to nearly 2100 (1960 return). From Figure 15 it can be seen that the 50 hPa Cl_y does not return to its 1960 value by the end of the 21st century outside the tropics. However, the beginning of the time series occurred for many CCMVal-2 models at about 1960 and some of the sensitivity found may be associated with model initialization. For example, a number of the models display increasing ozone in the early 1960s prior to their decrease in the 1970s and 1980s (e.g., see Figures 3 and 5). In these models ozone returns to 1960 values both prior to, and after the main loss near year 2000. In these cases the earlier return date was discarded and the later value used. This would appear to be a model spin-up issue.

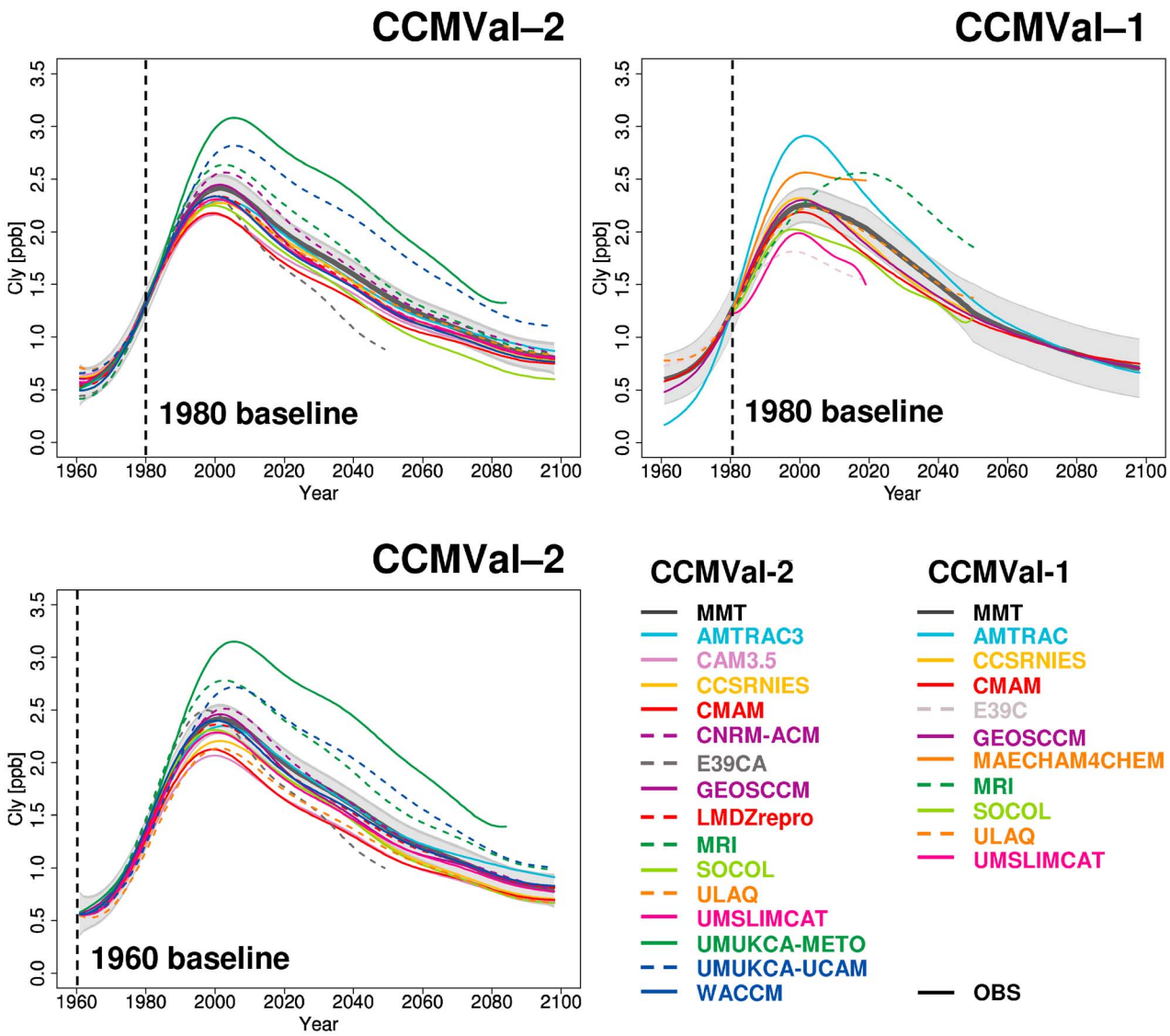

Figure 10. Same as Figure 2 but for 50 hPa Cl_y in the latitude range 60°N–90°N.

5.2. Relationship Between O_3 and Cl_y Return Dates

[34] Figure 16 shows the relationship between return date of 50 hPa Cl_y and column ozone back to their 1980 values using the MMT results. For the Antarctic spring, the models scatter approximately evenly about a similar date for the return of ozone and chlorine to 1980 values (given by the black line), indicating that halogen chemistry is the dominant factor in determining ozone recovery. Two models (CCSRNIES and UMUKCA-UCAM) fall significantly above the line, implying ozone returns faster than Cl_y, and several others fall significantly below the line, implying that ozone returns more slowly than Cl_y. The reason for these differences has not been identified, but may reflect in part the fact that in most models ozone recovers slowly in the middle 21st century, so that small ozone variations can cause a large change in ozone return date. A different picture is seen for the Arctic spring, and annual mean midlatitudes where most models return to 1980 column ozone values before Cl_y returns to 1980 values. As indicated in section 4.1, only about half of the models indicate a return of tropical ozone to the 1980 values. See also *Oman et al.* [2010], who calculate separate return dates for ozone columns above 20 hPa and 500–20 hPa.

5.3. Ozone Recovery as a Function of Latitude and Reference Date

[35] A complementary view of ozone recovery is shown in Figure 17, which indicates the return date of the model mean for the annual mean column ozone on the reference date given on the abscissa. E39CA has been excluded from the mean because of its short integration. The column has been separated into two regions, above and below 20 hPa, and the analysis excludes the atmosphere below 500 hPa. For

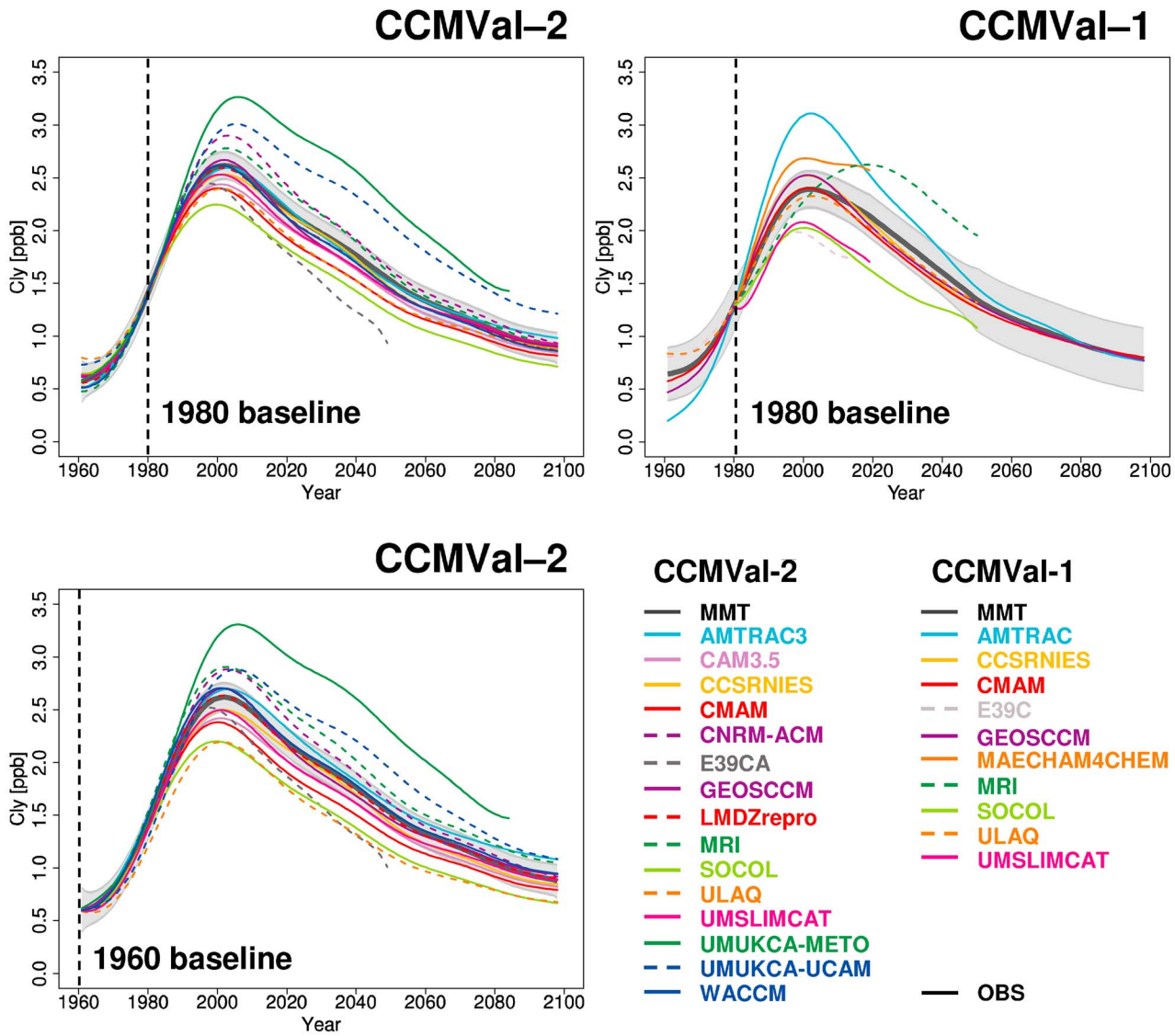

Figure 11. Same as Figure 2 but for 50 hPa Cl_y in the latitude range 60°S–90°S.

each year in the analysis the first date that ozone returned to the value on the reference date was determined for the mean model results. Above 20 hPa (Figure 17, top), ozone recovery is simulated to occur steadily. In this region, the temperature and chlorine effects on ozone dominate, as shown by the multilinear regression analysis of *Oman et al.* [2010]. As suggested by this analysis, ozone change is approximately linearly dependent on chlorine. Taking approximate values for Cl_y of 3, 1.5 and 0.75 ppbv for 2000, 1980 and 1960 implies that the ozone recovery from the peak depletion to 1960 levels should take about 50% longer than the recovery to 1980 levels. This is confirmed by Figure 17 (top).

[36] In the lower stratosphere (Figure 17, middle), as in Figure 14, a return date could not be established for the tropics due to the strengthening Brewer-Dobson circulation which systematically decreases tropical ozone as the simulations proceed [*Shepherd*, 2008; *Li et al.*, 2009; *Waugh et al.*, 2009]. The results also show a strong hemispheric asymmetry discussed in section 4.1, with Antarctic ozone recovering much more slowly than Arctic ozone. Again, this is due to climate change, which for the models as a whole has much more influence on ozone in the Northern than the Southern Hemisphere [*Austin and Wilson*, 2006; *Shepherd*, 2008]. In high southern latitudes, the simulations on average do not return to the pre-1970 ozone levels before the end of the simulations.

[37] The results for the total column (Figure 17, bottom) combine the results for the two regions. In the tropics, the total ozone column increases until about 2050 (Figure 1) due to decreasing halogen amounts and stratospheric cooling, but thereafter ozone decreases due to the increasing Brewer-Dobson circulation. This implies that in the tropics, the total ozone column does not return to pre-1985 values before the end of the simulations. Over Antarctica, recovery to 1960s levels of total ozone does not occur in the mean model until shortly before the end of the simulations.

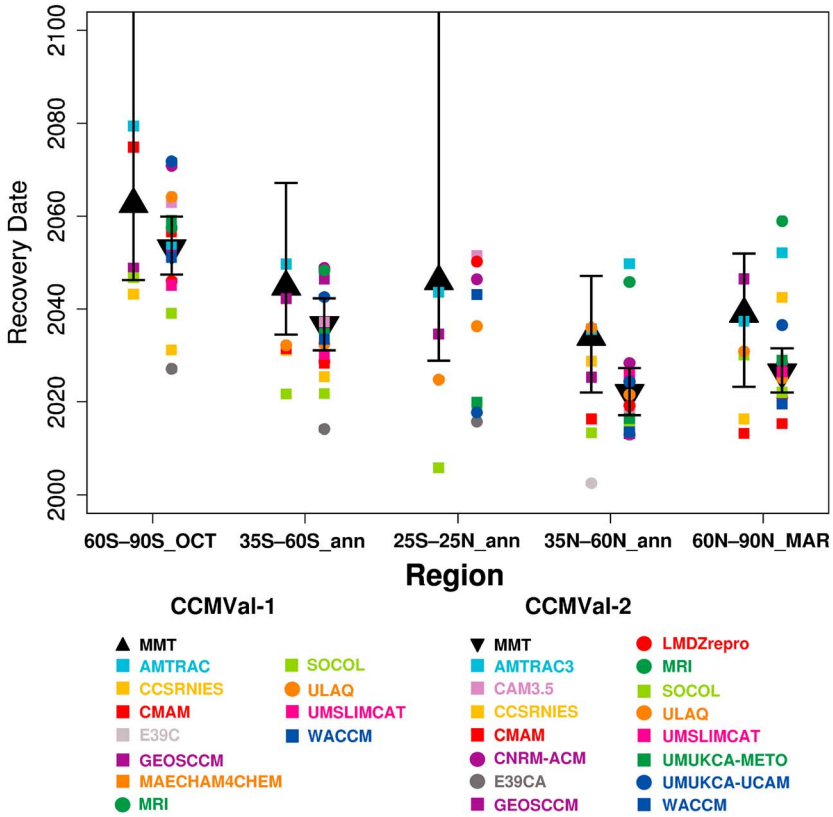

Figure 12. Date of return to 1980 values for the annual average (tropical and midlatitude) and spring (polar) total ozone column derived from the IMT (colored symbols) and MMT (large black triangles) estimates for CCMVal-1 and CCMVal-2 (left and right entries, respectively, in each latitude band). The error bars on the MMT estimate of return date is derived from the 95% confidence interval of the MMT estimates to the 1980 baseline-adjusted time series data.

5.4. Role of Transport in Midlatitude Ozone Recovery

[38] The role of transport in ozone recovery was examined by analyzing the seasonal cycle. The midlatitude total ozone column was first reconstructed using a least squares fit:

$$O_3(t) = \sum_{i=0}^{4} A_i \sin(i2\pi t) + B_i \cos(i2\pi t). \quad (1)$$

O_3 is the monthly and zonally average column ozone, averaged over the latitude range 35°–60° for each hemisphere, t is the time in years since the beginning of the period over which the seasonal cycle is fit, and A_i and B_i are the coefficients of the fit. The analysis was completed for 1960–1979 and 2040–2059. The periods were chosen as they corresponded to the time when halogen changes had a smaller effect on the ozone amount than at other times. The annual cycle derived from the fitting, with the annual mean for each model and time period removed is shown in Figures 18a and 18b (north) and 18d and 18e (south). These results are outside the main ozone hole period and show in both hemispheres a maximum in spring and a minimum in fall. Figures 18c and 18f show the changes in ozone seasonal cycle for the North and South between the two periods analyzed. The contrast between the two hemispheres can be seen in the seasonal cycle of the multimodel mean, shown by the solid black line in Figure 18, for which the increase in the springtime peak in the Northern Hemisphere is approximately twice as large as the change in the Southern Hemisphere (+3.5 DU versus +1.7 DU).

[39] Several models (notably ULAQ, GEOSCCM, CMAM and, to a lesser extent, WACCM) show an increased buildup of ozone through the boreal spring (Figure 18c). In contrast, other models (AMTRAC3, MRI and UMUKCA-METO) show little change in the amplitude of the seasonal cycle between these periods. Several models (CNRM-ACM, MRI and UMSLIMCAT) also show an increased buildup of ozone during Southern Hemisphere late fall and winter (May, June and July) (Figure 18f), but no coherent changes persist into the spring. The seasonal cycle is further perturbed with the breakup of the Antarctic vortex in October and November, mixing ozone depleted air from within the Antarctic vortex into midlatitudes.

[40] Figure 19 shows the relationship between the ozone seasonal cycle calculated as above, but averaged over late winter and spring and the MMT estimate of 1980 return date from the TSAM analysis (Figure 12). The models showing an increased buildup of ozone through the northern spring have midlatitude ozone return dates prior to 2020. In comparison, the models showing little change in the amplitude

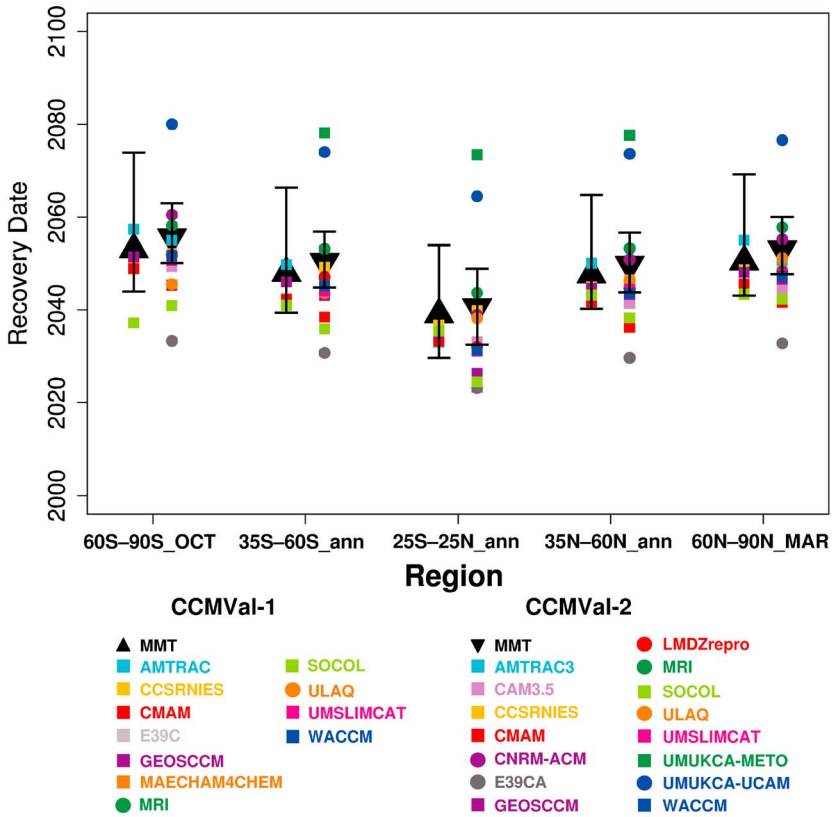

Figure 13. Date of return to 1980 values for the annual average 50 hPa Cl_y derived from the IMT (colored symbols) and MMT (large black triangles) estimates for CCMVal-1 and CCMVal-2 (left and right entries, respectively, in each latitude band). The error bars on the MMT estimate of return date is derived from the 95% confidence interval of the MMT estimates to the 1980 baseline-adjusted time series data.

of the seasonal cycle have return dates between 2040 and 2050. The UMUKCA-METO model is an exception, showing little change in the amplitude of the seasonal cycle yet having a return date before 2020. In contrast, no clear relationship can be found between changes in the springtime buildup of ozone and the return date in the Southern Hemisphere (Figure 19, right).

[41] Although chemistry affects the distribution of ozone, the springtime buildup of ozone is a feature in the annual cycle driven by the transport of ozone from tropical to middle latitudes by the Brewer-Dobson circulation [e.g., *Fusco and Salby*, 1999; *Fioletov and Shepherd*, 2003]. For this reason, combined with the fact that the seasonal chemical change is similar in both cases, changes in the springtime ozone column in Figures 18 and 19, are indicative of changes in transport in the models. For the Southern Hemisphere, the lack of a clear signal in the amplitude of the seasonal cycle of column ozone is evidence of a weaker change in the Southern Hemispheric branch of the strength of the Brewer-Dobson circulation and hence there is a smaller impact of transport on ozone return date.

6. Discussion

[42] The statistical interpretation used here and by *Scinocca et al.* [2010] is a considerable advance over that previously completed for IPCC or CCMVal. Clearly, we can only make inferences on the basis of the known uncertainties, and so the uncertainties are only estimates. We cannot account for processes that we do not know about. We do not consider it the role of our paper to resolve these issues, but rather see this as important work for the individual groups to pursue in order to obtain future model simulations which compare better with each other and with observations, to provide more confidence in the results of future multi-model assessments.

6.1. Uncertainties Related to the TSAM Method

[43] An important point for discussion is the confidence that can be attached to the TSAM analyses obtained. All the models ran essentially the same experiment and so may be treated as the same statistical sample. Each model was given the same weighting in the analysis. In principle, each model could have been weighted according to some criterion of model performance, such as its ability to simulate the strength of the polar vortex. Generally, though, for specific diagnostics it has proved difficult to decide how to assign weights with a degree of confidence. Also, there was substantial variation between the models even though some models share common roots [*Morgenstern et al.*, 2010]. Hence in practice, the multimodel mean was relatively insensitive to the weighting of the models.

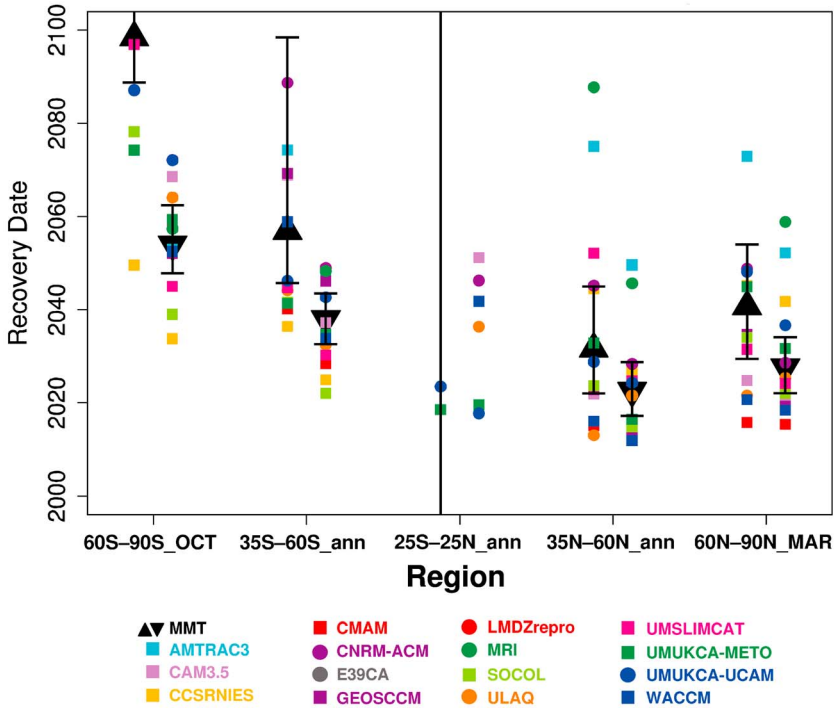

Figure 14. Date of return to 1960 (left entries) and 1980 (right entries) values for the annual average (tropical and midlatitude) and spring (polar) total ozone column derived from the IMT (colored symbols) and MMT (large black triangles) estimates for CCMVal-2. Error bars are as in Figure 13.

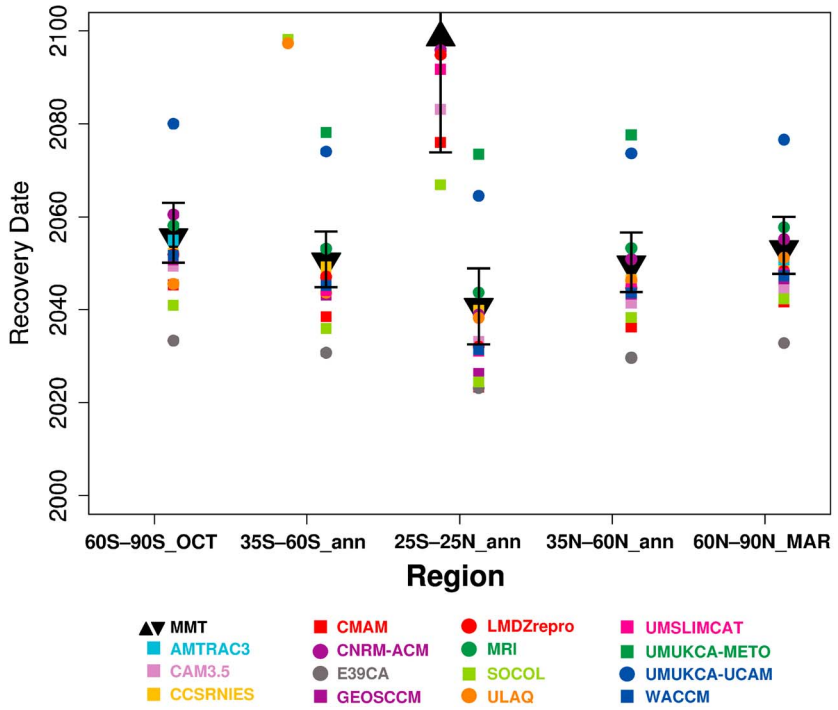

Figure 15. Date of return to 1960 (left entries) and 1980 (right entries) values for the annual average 50 hPa Cl_y derived from the IMT (colored symbols) and MMT (large black triangles) estimates for CCMVal-2. Error bars are as in Figure 13.

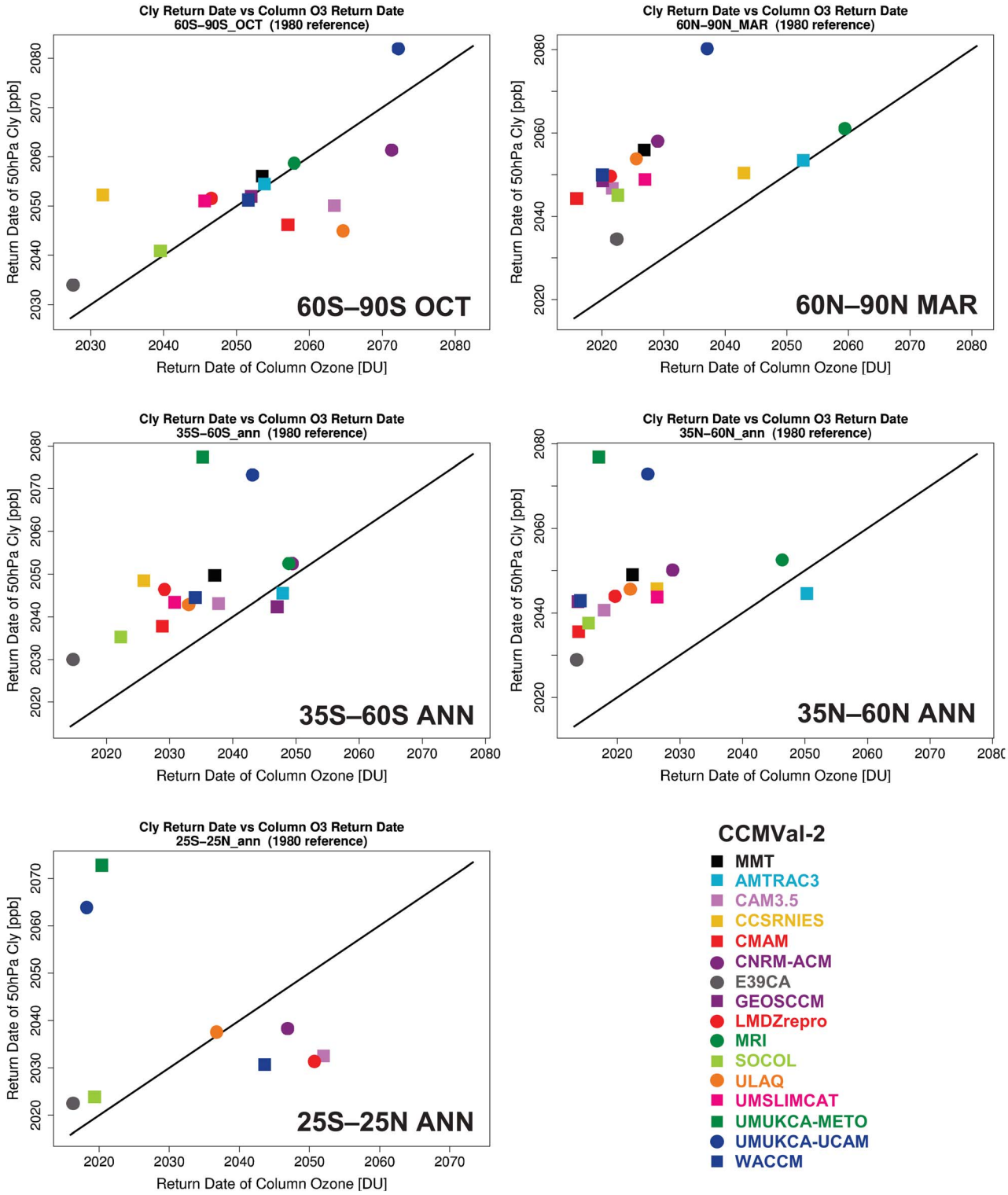

Figure 16. Relationship between the date of return of Cl_y to the 1980 value compared with the date of return of column ozone for the selected latitude ranges in Figure 13. Results are taken from the IMT and MMT fits.

[44] Over time one might expect model simulations to converge. This could follow usefully as a result of improved scientific understanding, or less usefully, as a tendency for modelers to duplicate physical parameterizations. In practice, there is no sign of a significant increase in convergence of model results over the last 4 years (the comparison between CCMVal-1 and CCMVal-2) as a result of for example the common roots in certain models. Improvements have arisen primarily from a consistency in the experiment period and the removal of known errors in earlier model versions.

6.2. Uncertainties Related to Forcings

[45] The purpose of CCMVal was to complete model intercomparisons which had the same GHG and CFC scenarios. As a result, the TSAM uncertainties indicated here cannot include any uncertainties in future scenarios. However, the models simulate a variety of results despite many common themes. Therefore the uncertainty in the processes indicated are reflected at least in part by the performance of the schemes in the models. For example, the SSTs used in the models are not identical, since they are, in most cases, those simulated by the core climate model, and in the case of one model the simulations have a coupled ocean. Consequently, the results include some variations due to uncertainties in future SSTs.

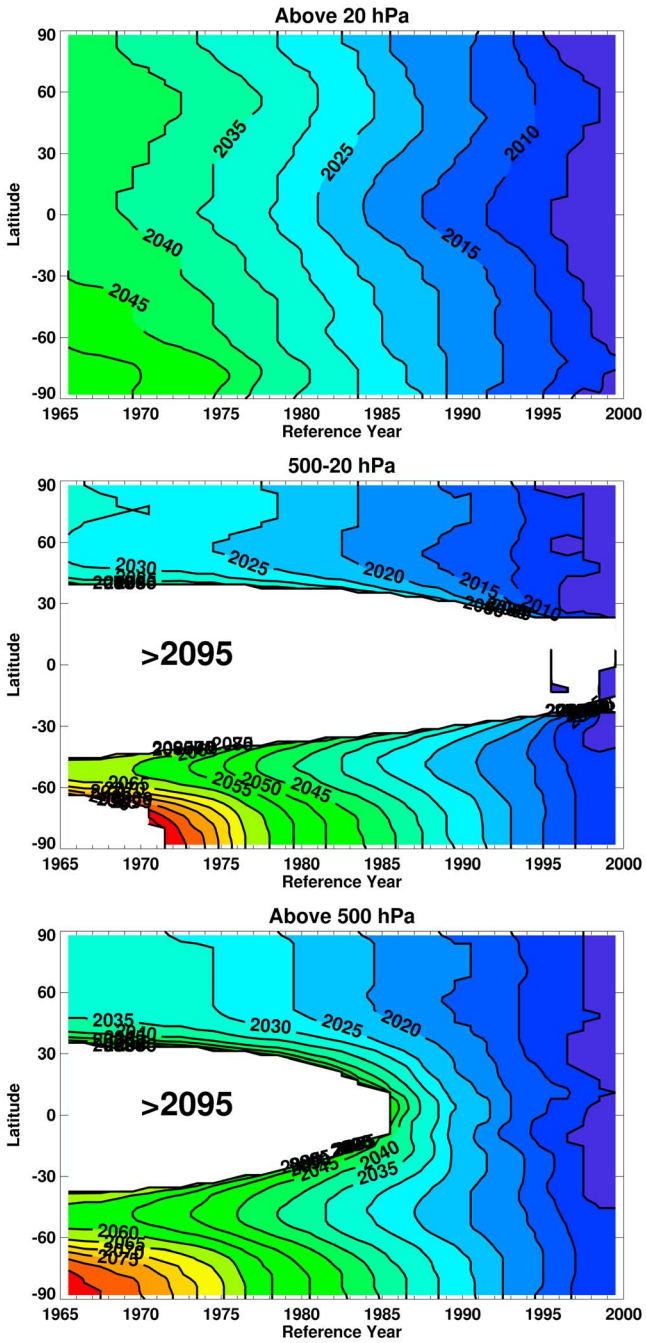

Figure 17. Date of return of the annual mean ozone to the value appropriate to the reference year indicated on the abscissa. Results were taken from the models AMTRAC3, CAM3.5, CCSRNIES, CMAM, CNRM-ACM, GEOSCCM, LMDZrepro, MRI, SOCOL, ULAQ, UMSLIMCAT, UMUKCA-UCAM, UMUKCA-METO, and WACCM, which were first interpolated to a common latitudinal grid (AMTRAC3). The model mean result was then smoothed with an 11 year running mean filter. The recovery date was determined from the time mean data. For presentation purposes, the recovery date was smoothed with a 1-2-1 filter in latitude. Data prior to 1965 (which limits the definition of the reference year data) or after 2094 (which limits the data for the return year) do not exist because of the need for an accurate time-smoothed field. The white region indicates where the mean model ozone has not recovered by the end of the simulations (nominally 2094). Results are shown (bottom) for the total column above 500 hPa, (middle) for the range 500–20 hPa, And (top) for the column above 20 hPa.

6.3. Uncertainties Due to Model Scientific Performance

[46] Naturally, model performance will vary between different regions and indeed different periods. We do not make a strong case for the model performance of Arctic polar loss: the multimodel mean could easily be strongly biased. This is critically dependent on lower stratospheric temperature which is difficult to simulate accurately. Moreover, there is sufficient interannual variability due to the model dynamics that even with a perfect model we could not be certain of simulating the observed trends. These uncertainties are reflected in the large differences between models. Whatever biases remain in polar ozone, the model results represent the best that can be obtained with current understanding. Other processes could be affected by basic model attributes such as upper boundary position or spatial resolution. Only one model had a low top, and only one model is clearly of lower horizontal resolution than the other models. These particular results would have had a small impact on the multimodel mean. Moreover, the performance of individual models could not in general be related to known model weaknesses. For example another model had neither a low top, nor low horizontal resolution and apparently accurate chemistry yet its ozone was still biased high compared with most models.

7. Summary

[47] A time series additive model (TSAM) analysis has been used to make individual and multimodel trend esti-

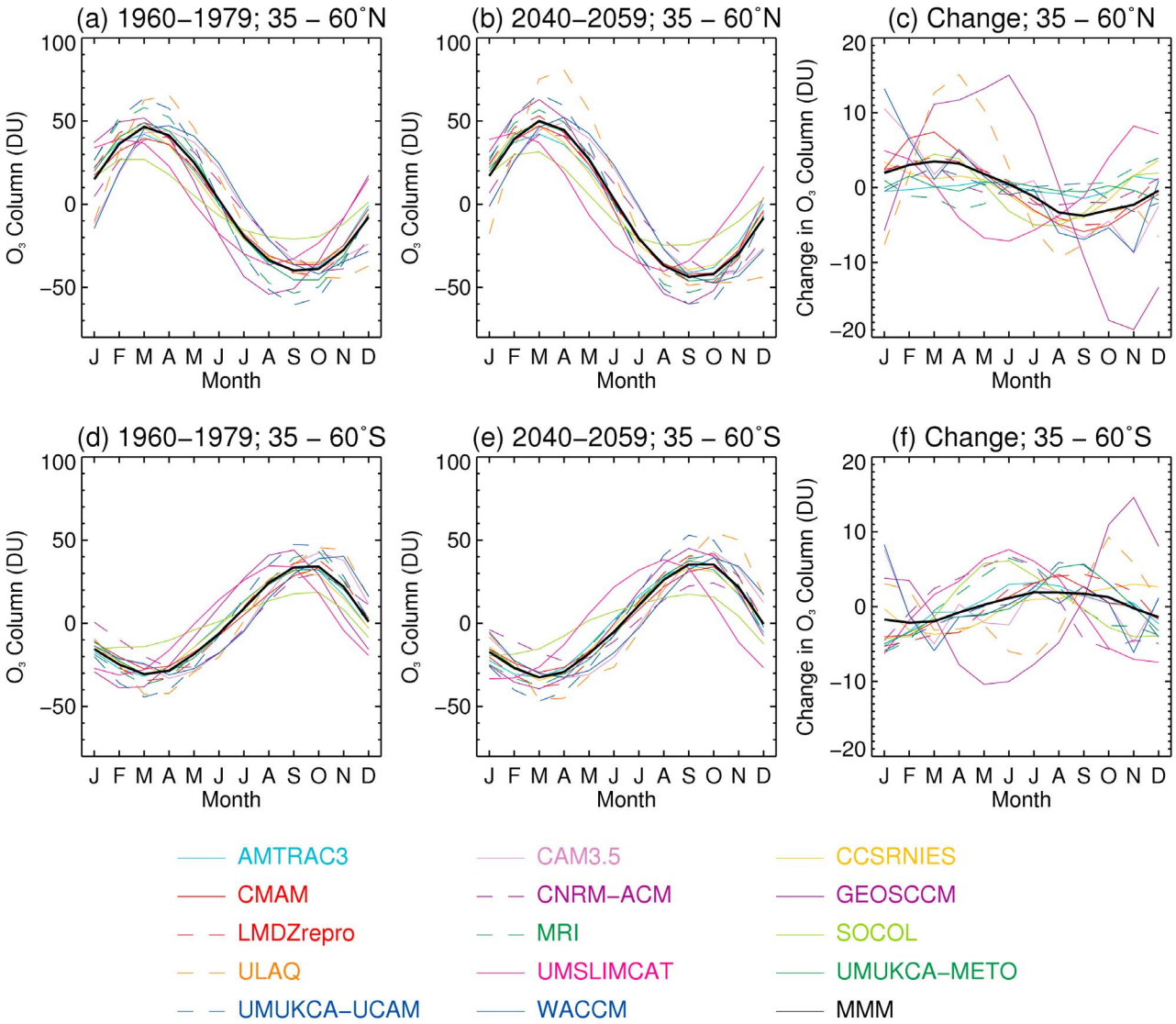

Figure 18. The average seasonal cycle of total column ozone (DU) over Northern and Southern Hemisphere midlatitudes for two periods and its change. (a) 1960–1979, 35°N–60°N, (b) 2040–2059, 35°N–60°N, (c) change from 1960–1979 to 2050–2059. (d, e, f) Same as Figures 18a, 18b, and 18c, respectively, but for the southern midlatitudes. The black curves indicated by MMM denote the multimodel mean. Note that the annual mean for each model and each time period is removed from the annual cycle before plotting and before taking the difference.

mates, which may be used to make rigorous statistical inferences. One of the main goals of this analysis was to produce quantitative multimodel ozone projections with associated uncertainty estimates. Another goal was the careful comparison of ozone projections between the CCMVal-1 and CCMVal-2 data sets to identify areas where models have improved and areas that continue to require modeling effort. In the application of the TSAM analysis it is clear that there are a number of practical issues that can influence this comparison (e.g., longer, more complete time series of the period of interest were submitted to CCMVal-2 compared to CCMVal-1).

[48] Overall, the model results obtained in CCMVal-2 were similar to those obtained in CCMVal-1. Although the model spread in the two assessments was similar, due in part to more models being available in CCMVal-2, more confidence can be attached to the results obtained. This is because for the CCMVal-2 models several factors have been improved, including a general improvement in Cl_y amounts. As a result, the differences in chlorine amount had less influence on ozone than in CCMVal-1 and the differences in model results were less dependent on those differences. Consequently, other processes, such as the strength of the circulation and possibly the temperature-dependent chemistry are likely playing a relatively greater role in the differences between model results.

[49] Other important differences in the two assessments were the earlier starting date of the simulations in CCMVal-2

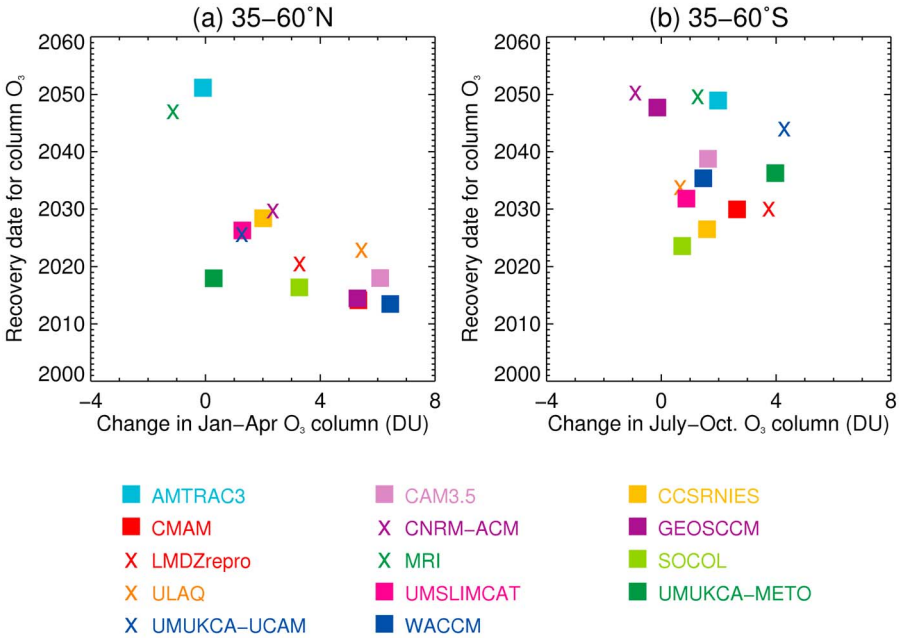

Figure 19. The relationship between the 1980 return date of midlatitude (35°–60°) annual average ozone from the MMT analysis and the change in amplitude of the seasonal cycle of ozone averaged over the spring in each hemisphere. The change in the seasonal cycle is defined as the difference between 1960–1979 and 2040–2059 and is shown in Figures 18b and 18d. The averages are calculated for January–April and July–October for the Northern and Southern Hemispheres, respectively.

and the fact that a large majority of the simulations covered the full 1960–2100 period of special interest. Even then, because of the likelihood of some ozone loss prior to 1970, it would in future be preferable to start simulations as early as 1950 (as several modeling groups did) in order to allow for model initialization issues.

[50] The TSAM analysis provided increased statistical confidence in the results obtained. In particular it is clear that the models simulate a hemispheric asymmetry in the timing for ozone to return to historical levels. By contrast chlorine amounts are projected to reduce at about the same rates independent of latitude. The conclusion is that other processes, in particular changes in greenhouse gas concentrations have contributed to ozone increase in accordance with previous work [e.g., *Austin and Wilson*, 2006; *Eyring et al.*, 2007; *Shepherd*, 2008; *Waugh et al.*, 2009]. It is therefore possible to encompass climate change processes within the definition of "ozone recovery," as we have done in this work. The results obtained here indicate that in the Northern Hemisphere extratropics, ozone would be expected to recover to 1980 levels about 20 years ahead of chlorine reduction to 1980 levels. In the Southern Hemisphere midlatitudes, ozone recovery is simulated to be slightly faster than chlorine (about 10 years) and in high latitudes, the timing of ozone recovery is driven primarily by chlorine (and bromine) amounts. Ozone recovery to 1960s levels is simulated to occur by about 2045 in the Northern Hemisphere, but as late as 2060 in southern midlatitudes or later than 2085 over the South Pole.

[51] One significant area of difference with CCMVal-1 is the lack of ozone recovery (according to the above-mentioned ozone recovery definition) in the tropics in the CCMVal-2 simulations. Although in the tropics ozone changes are small, transport, i.e., upward motion, is nonetheless likely to be the largest influence on column ozone. As a result simulated ozone decreases in the past (consistent with observations), and recovers slightly due to chlorine decreases. In the second half of the 21st century, column ozone is expected to reduce once more, primarily due to the transport effect dominating chlorine reduction, which is essentially complete.

[52] In this work we have investigated results from many models, but based on a single GHG scenario. Nonetheless, there is a need for a range of simulations looking at all aspects of the atmosphere-ocean system to try to address some of these issues. Uncertainties in net temperature changes, which arise from uncertainties in the increase of the strength of the Brewer-Dobson circulation versus radiative changes, need to be reduced. Realistic bromine amounts need to be included in model simulations to allow for the short lifetime species known to be present [*WMO*, 2007, chapter 2]. Finally, simulations with fixed halogens or fixed GHGs need to be completed to complement the realistic simulations that have been completed to establish more rigorously the impact of climate and chemistry changes on ozone.

[53] **Acknowledgments.** CCSRNIES research was supported by the Global Environmental Research Fund of the Ministry of the Environment of Japan (A-071). The MRI and CCSRNIES simulations were completed with the supercomputer at the National Institute for Environmental Studies, Japan. CMAM simulations were supported by CFCAS through the C-SPARC project. The Niwa-SOCOL and UMETRAC simulations were

supported by the New Zealand Foundation for Research, Science and Technology under contract C01X070. The UMSLIMCAT work was supported by NERC. The contribution of the Met Office Hadley Centre was supported by the Joint DECC and Defra Integrated Climate Programme, DECC/Defra (GA01101). The scientific work of the European CCM groups was supported by the European Commission through the project SCOUT-O3 under the 6th Framework Programme. J.A.'s research was administered by the University Corporation for Atmospheric Research at the NOAA Geophysical Fluid Dynamics Laboratory. Larry Horowitz and Dan Schwarzkopf provided useful comments on the paper. We acknowledge the Chemistry-Climate Model Validation (CCMVal) Activity for WCRP's (World Climate Research Programme) SPARC (Stratospheric Processes and their Role in Climate) project for organizing and coordinating the model data analysis activity, and the British Atmospheric Data Center (BADC) for collecting and archiving the CCMVal model output.

References

Akiyoshi, H., L. B. Zhou, Y. Yamashita, K. Sakamoto, M. Yoshiki, T. Nagashima, M. Takahashi, J. Kurokawa, M. Takigawa, and T. Imamura (2009), A CCM simulation of the breakup of the Antarctic polar vortex in the years 1980–2004 under the CCMVal scenarios, *J. Geophys. Res.*, *114*, D03103, doi:10.1029/2007JD009261.

Austin, J., and R. J. Wilson (2006), Ensemble simulations of the decline and recovery of stratospheric ozone, *J. Geophys. Res.*, *111*, D16314, doi:10.1029/2005JD006907.

Austin, J., and R. J. Wilson (2010), Sensitivity of polar ozone to sea surface temperatures and halogen amounts, *J. Geophys. Res.*, doi:10.1029/2009JD013292, in press.

Austin, J., et al. (2003), Uncertainties and assessments of chemistry-climate models of the stratosphere, *Atmos. Chem. Phys.*, *3*, 1–27.

Austin, J., et al. (2010), Chemistry-climate model simulations of spring Antarctic ozone, *J. Geophys. Res.*, *115*, D18303, doi:10.1029/2009JD013577.

Bodeker, G. E., H. Shiona, and H. Eskes (2005), Indicators of Antarctic ozone depletion, *Atmos. Chem. Phys.*, *5*, 2603–2615.

Butchart, N., and A. A. Scaife (2001), Removal of chlorofluorocarbons by increased mass exchange between the stratosphere and troposphere in a changing climate, *Nature*, *410*, 799–802.

de Grandpré, J., S. R. Beagley, V. I. Fomichev, E. Griffioen, J. C. McConnell, A. S. Medvedev, and T. G. Shepherd (2000), Ozone climatology using interactive chemistry: Results from the Canadian Middle Atmosphere Model, *J. Geophys. Res.*, *105*(D21), 26,475–26,491, doi:10.1029/2000JD900427.

Déqué, M. (2007), Frequency of precipitation and temperature extremes over France in an anthropogenic scenario: model results and statistical correction according to observed values, *Global Planet. Change*, *57*, 16–26.

Douglass, A. R., R. S. Stolarski, M. R. Schoeberl, C. H. Jackman, M. Gupta, P. A. Newman, J. E. Nielsen, and E. L. Fleming (2008), Relationship of loss, mean age of air and the distribution of CFCs to stratospheric circulation and implications for atmospheric lifetimes, *J. Geophys. Res.*, *113*, D14309, doi:10.1029/2007JD009575.

Eyring, V., et al. (2006), Assessment of temperature, trace species, and ozone in chemistry-climate model simulations of the recent past, *J. Geophys. Res.*, *111*, D22308, doi:10.1029/2006JD007327.

Eyring, V., et al. (2007), Multi-model projections of ozone recovery in the 21st century, *J. Geophys. Res.*, *112*, D16303, doi:10.1029/2006JD008332.

Eyring, V., et al. (2008), Overview of the new CCMVal reference and sensitivity simulations in support of the upcoming ozone and climate assessments and the planned SPARC CCMVal, *SPARC Newsl.*, *30*, 20–26.

Fioletov, V. E., and T. G. Shepherd (2003), Seasonal persistence of mid-latitude total ozone anomalies, *Geophys. Res. Lett.*, *30*(17), 1417, doi:10.1029/2002GL016739.

Fioletov, V. E., G. E. Bodeker, A. J. Miller, R. D. McPeters, and R. Stolarski (2002), Global ozone and zonal total ozone variations estimated from ground-based and satellite measurements: 1964–2000, *J. Geophys. Res.*, *107*(D22), 4647, doi:10.1029/2001JD001350.

Fusco, A. C., and M. L. Salby (1999), Interannual variations of total ozone and their relationship to variations of planetary wave activity, *J. Clim.*, *12*, 1619–1629.

Garcia, R. R., D. R. Marsh, D. E. Kinnison, B. A. Boville, and F. Sassi (2007), Simulation of secular trends in the middle atmosphere, 1950–2003, *J. Geophys. Res.*, *112*, D09301, doi:10.1029/2006JD007485.

Garny, H., M. Dameris, and A. Stenke (2009), Impact of prescribed SSTs on climatologies and long term trends in CCM simulations, *Atmos. Chem. Phys.*, *9*, 6017–6031.

Holton, J. R., and H.-C. Tan (1980), The influence of the equatorial quasi-biennial oscillation on the global circulation at 50mb, *J. Atmos. Sci.*, *37*, 2200–2208.

Intergovernmental Panel on Climate Change (IPCC) (2001), *Climate Change 2001: the Scientific Basis. Contribution of Working Group I to the Third Assessment Report*, edited by J. T. Houghton et al., 881 pp., Cambridge Univ. Press, Cambridge, U. K.

Jourdain, L., S. Bekki, F. Lott, and F. Lefèvre (2008), The coupled chemistry-climate model LMDz-REPROBUS: description and evaluation of a transient simulation of the period 1980–1999, *Ann. Geophys.*, *26*, 1391–1413.

Lamarque, J.-F., D. E. Kinnison, P. G. Hess, and F. M. Vitt (2008), Simulated lower stratospheric trends between 1970 and 2005: Identifying the role of climate and composition changes, *J. Geophys. Res.*, *113*, D12301, doi:10.1029/2007JD009277.

Li, F., R. S. Stolarski, and P. A. Newman (2009), Stratospheric ozone in the post-CFC era, *Atmos. Chem. Phys.*, *9*, 2207–2213.

Miller, A. J., et al. (2002), A cohesive total ozone data set from SBUV(/2) satellite system, *J. Geophys. Res.*, *107*(D23), 4701, doi:10.1029/2001JD000853.

Morgenstern, O., P. Braesicke, F. M. O'Connor, A. C. Bushell, C. E. Johnson, S. M. Osprey, and J. A. Pyle (2009), Evaluation of the new UKCA climate-composition model—Part 1: The stratosphere, *Geosci. Model Dev.*, *2*, 43–57.

Morgenstern, O., et al. (2010), A review of CCMVal-2 models and simulations, *J. Geophys. Res.*, *115*, D00M02, doi:10.1029/2009JD013728.

Oman, L., et al. (2010), Multimodel assessment of the factors driving stratospheric ozone evolution over the 21st century, *J. Geophys. Res.*, doi:10.1029/2010JD014362, in press.

Pawson, S., R. S. Stolarski, A. R. Douglass, P. A. Newman, J. E. Nielsen, S. M. Frith, and M. L. Gupta (2008), Goddard Earth Observing System chemistry-climate model simulations of stratospheric ozone-temperature coupling between 1950 and 2005, *J. Geophys. Res.*, *113*, D12103, doi:10.1029/2007JD009511.

Pitari, G., E. Mancini, V. Rizi, and D. T. Shindell (2002), Impact of future climate and emission changes on stratospheric aerosols and ozone, *J. Atmos. Sci.*, *59*, 414–420.

Portmann, R. W., and S. Solomon (2007), Indirect radiative forcing of the ozone layer during the 21st century, *Geophys. Res. Lett.*, *34*, L02813, doi:10.1029/2006GL028252.

Schraner, M., E. Rozanov, and C. Schnadt-Poberaj (2008), Technical note: Chemistry-climate model SOCOL: version 2.0 with improved transport and chemistry/microphysics schemes, *Atmos. Chem. Phys.*, *8*, 5957–5974.

Scinocca, J. F., N. A. McFarlane, M. Lazare, J. Li, and D. Plummer (2008), The CCCma third generation AGCM and its extension into the middle atmosphere, *Atmos. Chem. Phys.*, *8*, 7055–7074.

Scinocca, J. F., D. B. Stephenson, T. C. Bailey, and J. Austin (2010), Estimates of past and future ozone trends from multimodel simulations using a flexible smoothing spline methodology, *J. Geophys. Res.*, doi:10.1029/2009JD013622, in press.

Shepherd, T. G. (2008), Dynamics, stratospheric ozone and climate change, *Atmos. Ocean*, *46*, 117–138.

Shibata, K., and M. Deushi (2008), Long term variations and trends in the simulation of the middle atmosphere 1980–2004 by the chemistry-climate model of the Meteorological Research Institute, *Ann. Geophys.*, *26*, 1299–1326.

Shine, K. P., et al. (2003), A comparison of model-simulated trends in stratospheric temperatures, *Q. J. R. Meteorol. Soc.*, *129*, 1565–1588.

Solomon, S. (1999), Stratospheric ozone depletion: A review of concepts and history, *Rev. Geophys.*, *37*, 275–316.

Stenke, A., M. Dameris, V. Grewe, and H. Garny (2009), Implications of Lagrangian transport for simulations with a coupled chemistry-climate model, *Atmos. Chem. Phys.*, *9*, 5489–5504.

Stolarski, R. S., and S. Frith (2006), Search for evidence of trend slowdown in the long-term TOMS/SBUV total ozone data record: The importance of instrument drift uncertainty, *Atmos. Chem. Phys.*, *6*, 4057–4065.

Takahashi, M. (1996), Simulation of the stratospheric quasi-biennial oscillation using a general circulation model, *Geophys. Res. Lett.*, *23*, 661–664.

Teyssèdre, H., et al. (2007), A new tropospheric and stratospheric Chemistry and Transport Model MOCAGE-Climat for multi-year studies: Evaluation of the present-day climatology and sensitivity to surface processes, *Atmos. Chem. Phys.*, *7*, 5815–5860.

Tian, W., and M. P. Chipperfield (2005), A new coupled chemistry-climate model for the stratosphere: The importance of coupling for future O_3-climate predictions, *Q. J. Meteorol. Soc.*, *131*, 281–303.

Tie, X., and G. Brasseur (1995), The response of stratospheric ozone to volcanic eruptions: Sensitivity to atmospheric chlorine loading, *Geophys. Res. Lett.*, *22*, 3035–3038, doi:10.1029/95GL03057.

Waugh, D. W., L. Oman, S. R. Kawa, R. S. Stolarski, S. Pawson, A. R. Douglass, P. A. Newman, and J. E. Nielsen (2009), Impact of climate change on stratospheric ozone recovery, *Geophys. Res. Lett.*, *36*, L03805, doi:10.1029/2008GL036223.

World Meteorological Organization (WMO) (2007), Scientific assessment of ozone depletion: 2006, *Global Ozone Res. and Monit. Proj. Rep. 50*, Geneva, Switzerland.

H. Akiyoshi, T. Nakamura, and Y. Yamashita, National Institute for Environmental Studies, 16-2 Onogawa, Tsukuba, Ibaraki 305-8506, Japan.

J. Austin and R. J. Wilson, Geophysical Fluid Dynamics Laboratory, NOAA, Princeton, NJ 08542-0308, USA. (john.austin@noaa.gov)

S. Bekki, D. Cugnet, and M. Marchand, LATMOS, IPSL, UVSQ, UPMC, CNRS, INSU, F-75231 Paris, France.

P. Braesicke and J. Pyle, NCAS-Climate-Chemistry, Centre for Atmospheric Science, Department of Chemistry, Cambridge University, Cambridge CB2 IEW, UK.

N. Butchart and S. C. Hardiman, Hadley Centre, Met Office, Exeter EX1 3PB, UK.

M. Chipperfield and S. Dhomse, School of Earth and Environment, University of Leeds, Leeds LS2 9JT, UK.

M. Dameris, V. Eyring, and H. Garny, Deutsches Zentrum für Luft- und Raumfahrt, Institut für Physik der Atmosphäre, Wessling D-82234, Germany.

S. Frith and S. Pawson, NASA Goddard Space Flight Center, Greenbelt, MD 20771, USA.

R. R. Garcia, A. Gettelman, D. Kinnison, and J. F. Lamarque, NCAR, Boulder, CO 80305, USA.

E. Mancini and G. Pitari, Dipartimento di Fisica, University of L'Aquila, I-167100 L'Aquila, Italy.

M. Michou and H. Teyssèdre, GAME, CNRM, Meteo-France, F-31057 Toulouse, France.

O. Morgenstern, National Institute of Water and Atmospheric Research, Private Bag 50061, Omakau, Lauder, 9352, New Zealand.

L. Oman and D. Waugh, Department of Earth and Planetary Sciences, John Hopkins University, Baltimore, MD 21218, USA.

D. Plummer, Science and Technology Branch, Environment Canada, Toronto, ON M3H 5T4, Canada.

E. Rozanov, Physical-Meteorological Observatory, World Radiation Center, CH-7260 Davos, Switzerland.

J. Scinocca, CCMA, University of Victoria, Victoria, BC V8W 3V6, Canada.

T. G. Shepherd, Department of Physics, University of Toronto, Toronto, ON M5S 1A7, Canada.

K. Shibata, Meteorological Research Institute, Japan Meteorological Agency, Tsukuba, Ibaraki 305-0052, Japan.